The Farthest Point Map on the Regular Dodecahedron

Richard Evan Schwartz *

April 6, 2021

Abstract

Let X be the regular dodecahedron, equipped with its intrinsic path metric. Given $p \in X$ let $G(p) = -q$ where q is the point on X which maximizes the distance to p. (Generically, G is single-valued.) We give a complete description of the map G and as a consequence show that the ω-limit set of G is the 1-skeleton of a subdivision of X into 180 convex quadrilaterals. G is a piecewise bi-quadratic map, and each algebraic piece is defined by a straight line construction involving a rhombus. The rhombi involved have the same shapes as the ones in the Penrose tiling. Our proof is computer-assisted but rigorous.

1 Introduction

Let (X, d_X) be a compact metric space. The *farthest point map*, or *farpoint map* for short, associates to each point $p \in X$ the set $\mathcal{F}_p \subset X$ of points $q \in X$ which maximize the distance function $q \to d_X(p, q)$. When X is a the surface of a convex polyhedron we always take d_X to be the intrinsic metric measured in terms of paths on X rather than the chordal metric coming from $\boldsymbol{R}^3$. The farpoint map is pretty boring with respect to the chordal metric.

J. Rouyer's paper [**R1**] gives a complete description of the farthest point map on the regular tetrahedron. My recent paper [**S**] gives a complete description for the regular octahedron. The paper [**W**] has some results for

*Supported by N.S.F. Grant DMS-1807320

the case of centrally symmetric octahedra having all equal cone angles. The papers [**R2**], [**R3**] study the farthest point map for general convex polyhedra. The papers [**V1**], [**V2**], [**VZ**], and [**Z**] study the map on general convex surfaces.

Given the work in [**R1**] and [**S**], it is natural to wonder about what happens for the other platonic solids. The case of the cube and the icosahedron seem quite similar to that of the octahedron. The case of the dodecahedron is the most intricate and beautiful. I had originally planned to write about all cases at the same time, but the dodecahedron case already makes for a long story. This paper is a companion to a Java program I wrote, which shows all the structure. One can get this program on GitHub:

http://www.github.com/RichardEvanSchwartz/Dodecahedron

Henceforth X denotes the regular dodehahedron equipped with its intrinsic path metric. It is nicer to think about the set

$$\mathcal{G}_p = A(\mathcal{F}_p), \tag{1}$$

where A is the antipodal map. When $\mathcal{G}_p$ is a singleton, we define $G(p)$ to be this point. Whenever we write $G(p)$ we mean implicitly that $\mathcal{G}_p$ is a singleton.

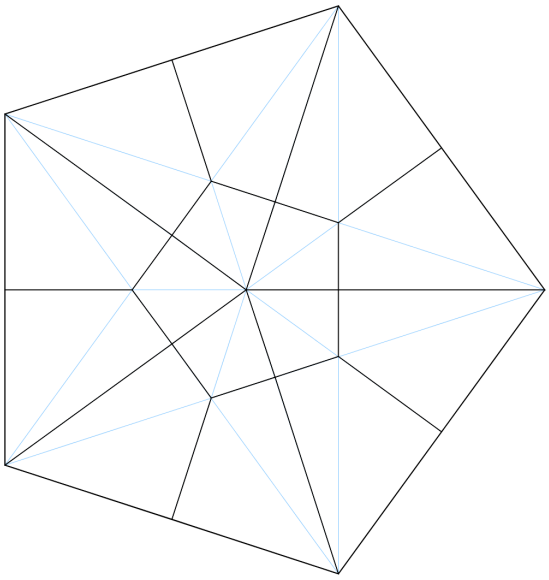

Figure 1.1: The decomposition of Π into states

Since G commutes with every isometry of X, it suffices to describe the action of G on a single pentagonal face Π of X. Henceforth we take our points in Π. We identify Π with the planar pentagon whose vertices are the 5th roots of unity. Figure 1.1 shows a subdivision of Π into 15 quadrilaterals, which we call *states*. The blue segments are drawn just as guides. The edges of the states are the black segments. Let $\mathcal{E}$ denote the union of the state edges.

Recall that the *ω-limit set* $L_\omega(G)$ of G is the accumulation set of the well-defined G-orbits. Here is a corollary of our main result.

Theorem 1.1 *$G(p) = p$ if and only if $p \in \mathcal{E}$, and $L_\omega(G) \cap \Pi = \mathcal{E}$.*

Now we turn towards describing our main result. We introduce a map which we call a *rhombus map*. A very similar map turned up in [**S**] though we did not study it as formally.

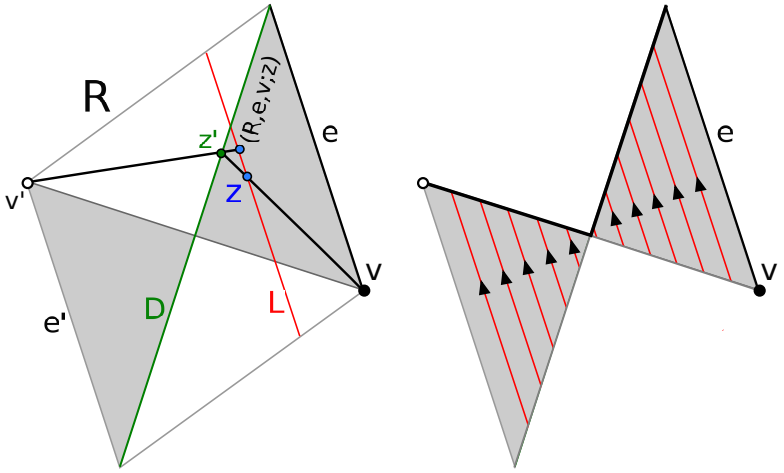

Figure 1.2: A rhombus map $z \to (R, e, v; z)$ and its invariant foliation.

A rhombus map is defined by a triple (R, e, v) where R is a rhombus, e is an edge of R, and v is a vertex of R incident to e. That is, (v, e) is a flag of R. Let (v', e') denote the opposite flag. Let D be the diagonal of R that does not contain v. Let R^o be the interior of R. Given $z \in R^o$ let L_z be the line parallel to e through z. We define

$$(R, e, v; z) = \overline{v'z'} \cap L_z, \qquad z' = \overline{vz} \cap D. \tag{2}$$

Our map carries z to $(R, e, v; z)$. Figure 1.2 shows the construction.

We take the domain of (R, e, v) to be the union R^* of the open shaded triangles in Figure 1.2. The map (R, e, v) is a bi-quadratic self-diffeomorphism of R^* which fixes $\partial R^* - (e \cup e')$ pointwise. The restriction of (R, e, V) to each segment of R^* parallel to e is a real projective automorphism. We foliate R^* by these segments. The orbits of (R, e, v) move along the leaves of this foliation in direction pointing away from v. The attracting fixed point set of the (R, e, v) is the union of the two half-diagonals of R bounding the upper white triangle. The maps (R, e', v') and (R, e, v) are inverses of each other.

Example: We take $R = [-1, 1]^2$. and $v = (-1, -1)$ and e the vertical edge connecting $(-1, -1)$ to $(-1, 1)$. In this case, the map is given by

$$(R, e, v; (x, y)) = f(x, y) = \left(x, \frac{x^2 + y}{1 + y}\right). \tag{3}$$

Every rhombus map has the form $\psi \circ f \circ \psi^{-1}$ for some affine transformation ψ.

Figure 1.3 shows two special Rhombus maps which are relevant to the dodecahedron.

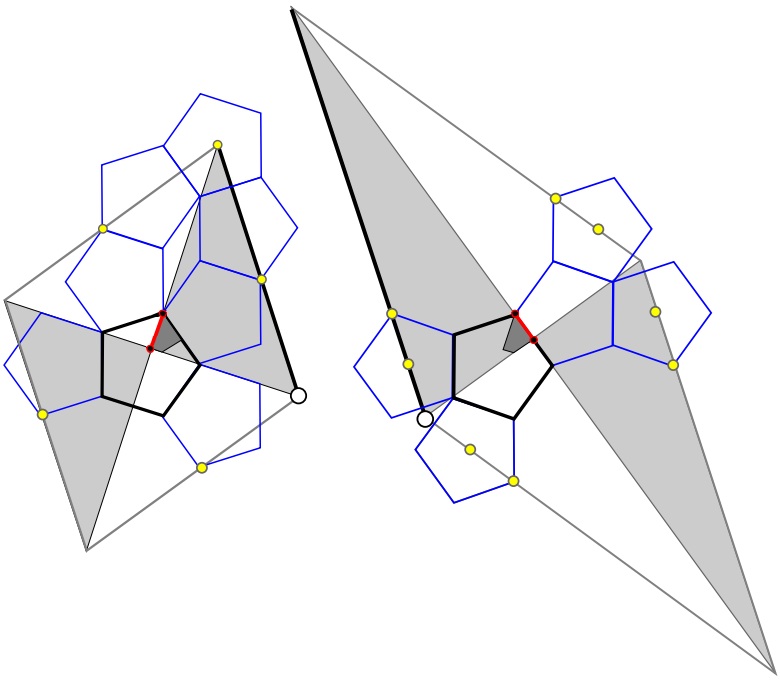

Figure 1.3: Two special rhombus maps

These rhombs have the same shapes as those in a Penrose tiling. The black central pentagons in Figure 1.3 are Π. The blue pentagons are scaffolding, designed to illustrate the construction of the rhombs. The darkly shaded regions in the black pentagon are states. Let $\mathcal{R}$ denote the smallest family of rhombus maps which contains these two and which is closed with respect to taking inverses and conjugating by the dihedral symmetry group of Π. The family $\mathcal{R}$ consists of 40 maps. We say that an $\mathcal{R}$-*map* is a map defined by one of the members of $\mathcal{R}$.

We say that a state Σ is *adapted* to a $\mathcal{R}$-map (R, e, v) if $\Sigma^o \subset R^*$ and if the diagonals of R contain two consecutive sides of Σ. Each state is adapted to 4 $\mathcal{R}$-maps, and the associated foliations all coincide. Thus we foliate Σ by parallel line segments by restricting the foliations of the associated maps. The state shown in Figure 1.3 is adapted to both of the $\mathcal{R}$-maps shown there. Each $\mathcal{R}$-map adapted to Σ *selects* the edge of Σ that is contained in the attracting fixed point set of the map. Each edge of Σ is selected by a unique adapted $\mathcal{R}$-map. The selected edges are red in Figure 1.3.

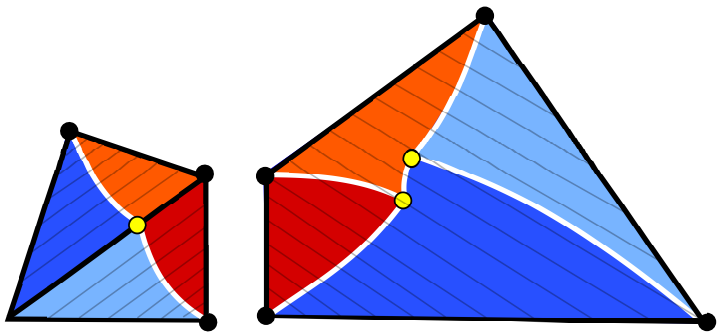

Figure 1.4: Combinatoral pattern in two of the cities.

We say that a *city* is a closed topological disk whose boundary is a union of 3 or 4 algebraic arcs which are either line segments or cubic curves. We call these segments/curves the *edges* of the city. Figure 1.4 shows a schematic decomposition of two of the states into 4 cities each. The decomposition on the left is meant to have bilateral symmetry. The white edges are nontrivial cubics and the black edges are line segments. We insist that each segment in the foliation of Σ intersects the union of edges at the red-blue interface exactly once. One edge of each city coincides with an edge of the state. We call these edges *external* and the rest *internal*. To each city we associate the unique $\mathcal{F}$-map which is adapted to the state and which selects the external edge of the city.

Theorem 1.2 *Let Σ be a state. Σ has a decomposition into 4 cities in the combinatorial pattern shown in Figure 1.4. If $p \in \Sigma$ then $\mathcal{G}_p$ is the union of the images of p under the $\mathcal{R}$-maps associated to the cities that contain p.*

Let us unpack and clarify this result. Each state is isometric to one of the two shown in Figure 1.4, so by "a decomposition", we mean whichever one in Figure 1.4 corresponds to the isometry type of the state. If $p \in \partial\Sigma$ then p is fixed by the one or two associated maps. Hence G is the identity on $\partial\Sigma$. If p lies in the interior of some city, then $G(p)$ is the image of p under the associated $\mathcal{R}$-map. Suppose that p lies in the interior of an edge e common to two cities. If e is incident to a non-right-angled vertex of Σ, then the two associated maps agree on p, and $G(p)$ is defined by either map. If e is incident to a right-angled vertex of Σ, then the two associated maps are inverses of each other and $\mathcal{G}_p$ is a pair of points. If $e \subset \Sigma^o$ then $\mathcal{G}_p$ consists of 2 points, not as clearly related to each other. If p lies 3 or more states, then then $\mathcal{G}_p$ is a pair of points.

Now we show what the cities actually look like. Figure 1.5 below shows the decomposition of Π into the 60 cities. One impressive thing about the picture is that the internal city edges are only straight line segments when they are contained in lines of bilateral symmetry of Π. Thus, the red-blue interfaces look like they are straight line segments joining non-adjacent edge midpoints of Π but this just an illusion. These are all arcs of irreducible cubic curves which have the general form given in Equation 4 below. My computer program lets you zoom in and see that they are not straight line segments.

To give a complete account of the farpoint map on X we need to give equations for the curves bounding the cities. The line segment edges are all part of the framework shown in Figure 1.1. The cubic edges are all solutions of equations of the following form

$$\sum_{i+j\le 3} \left(s_{ij}\sqrt{a_{ij}+b_{ij}\sqrt{5}} \right) x^i y^j = 0, \qquad s_{ij} \in \{-1,0,1\}, \quad a_{ij}, b_{ij} \in \boldsymbol{Z}. \quad (4)$$

We give the precise formulas in §8.4. The integers involved in the equations are sometimes surprisingly large. The coordinates for the yellow triple points in Figure 1.4, which we also list in §8.4, also have crazy equations.

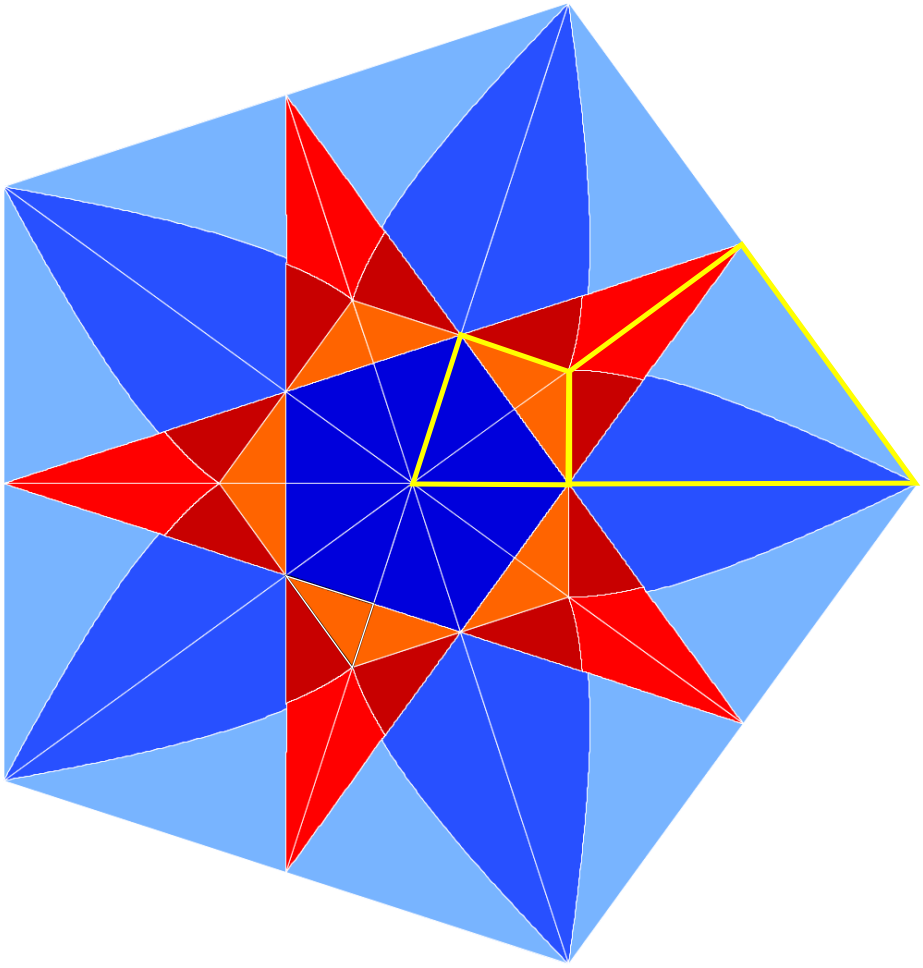

Figure 1.5: The decomposition into cities.

Proof of Theorem 1.1: We see immediately from the description in Theorem 1.2 that $G(p) = p$ if and only if p lies in an edge of a state. Now let us understand the ω-limit set. Inside the state Σ, the map G preserves the foliation by parallel line segments. Let σ be such a line segment. This segment intersects the red-blue interface at a single point p_σ. If $p \in \sigma - p_\sigma$ then G pushes p away from p_σ and towards the endpoint of σ. Thus the iterates $p, G(p), G^2(p), ...$ converge to one endpoint of σ or the other, depending on the side of $\sigma - p_\sigma$ which contains p. This shows that all orbits in σ accumulate on the endpoints of σ. But then we sweep out all of $\partial\Sigma$ as we vary σ within the foliation. ♠

Our proof of Theorem 1.2 follows a pattern similar to what we did in [**S**], though the details are much more involved. I don't completely understand the huge jump in complexity (of the proof) one sees when going from the regular octahedron to the regular dodecahedron but I think that a lot of it derives from the fact that the regular pentagon does not tile the plane whereas the equilateral triangle does. In the case of the octahedron we had a global tiling which we used in order to compare geodesic paths on the octahedron. Instead, we have something like a tree of possible combinatorial types associated to a geodesic segment on X, and we resort to a computer search to tame the huge number of combinatorial possibilities. To give an example, there are 70 distinct combinatorial ways that a length minimizing geodesic segment traveling from the bottom face of X to the top face of X can interact with the other faces of X.

Even after we narrow down the number of combinatorial types we need to consider, the algebra involved in the computations is formidible. Typically we consider cubic polynomials in 2 variables with coefficients in a degree 8 extension of $\boldsymbol{Q}$. These are not polynomials that one can just stare at and understand. We found it easiest to let Mathematica [**Wo**] deal with these polynomials in an automatic way. The main technical gadget that powers our proof is a positivity certificate for polynomials in two variables, *the positive dominance criterion*, which we discuss in §2.7.

I have to admit that I am disappointed at the length and complexity of the paper, and I may not try to publish it. However, I think it is worth having a complete proof of Theorem 1.2 on the record.

Here is an outline of the paper. In §2 we describe some preliminary notions, such as the developing map. In §3 we prove the main results modulo technical details. In §4-7 we fill in the details of the outline. Again, this is a heavily computer-assisted proof which freely makes use of the symbolic manipulation powers of Mathematica.

In addition to getting my Java program, the reader can also get my Mathematica code from the same GitHub address. The directory with the Mathematica code has an extensive README file explaining how to run the calculations.

I thank In-Jee Jeong and Nathan Dunfield for discussions about this paper. I thank the Simons Foundation for their support, in the form of a 2020-21 Simons Sabbatical Fellowship. Finally, I think the Institute for Advanced Study for their support, in the form of a 2020-21 membership funded by a grant from the Ambrose Monell Foundation.

2 Preliminaries

2.1 A Spatial Argument

As in the introduction, we let X denote the regular dodecahedron equipped with its intrinsic path metric. X is locally Euclidean except for 20 cone points. The cone points each have cone angle $9\pi/5$. As a polyhedron, X has 12 regular pentagonal *faces*. We identify one face Π of X with the regular pentagon whose vertices are the 5th roots of unity. We think of Π as being the bottom face. The antipodal face $A(\Pi)$ is the top face. Geometrically, we are normalizing so that the distance from the center of a face of X to a vertex of that face is 1 unit.

Almost all of our paper uses intrinsic 2-dimensional arguments, but there is one spatial argument we give, in order to shorten the overall proof. Let us do this first. Let $\phi = (1+\sqrt{5})/2$. The following facts are well known.

1. The diameter of any face of X is $1 + (\phi/2)$.

2. The sphere inscribed in X has radius $\phi^2/2$.

Lemma 2.1 *If $p \in \Pi$ then $\mathcal{F}_p$ is disjoint from the faces adjacent to Π.*

Proof: Suppose this is false, and $q \in \mathcal{F}_p$ is in a face adjacent to Π. By Fact 1, the points p and q may be connected to a path of length at most $2 + \phi < 4$. On the other hand, and path in X connecting p to $A(p)$ stays outside the inscribed sphere and has endpoints which are antipodally placed with respect to its center. Hence, $d_X(p, A(p)) \geq \pi\phi^2/2 > 4$. This proves that $A(p)$ is farther from p than is q. Hence $q \notin \mathcal{F}_p$. ♠

Remark: We will eventually show that $\mathcal{F}_p \subset A(\Pi)$, but a crude argument like the one above would not work work to rule out the possibility that $\mathcal{F}_p$ contains points in the interior of a face adjacent to $A(\Pi)$. The problem is that the vertex antipodal to any vertex of Π lies both in $A(\Pi)$ and an adjacent face.

Having finished with the spatial argument, we turn to more 2-dimensional considerations.

2.2 The Developing Map

Figure 2.1 shows a combinatorial diagram for X. We have $\Pi = \Pi_0$. The antipodal face $A(\Pi) = \Pi_{11}$ is not shown. We have colored the faces of X according to their combinatorial distance from Π. In the pictures below we will color Π_{11} red.

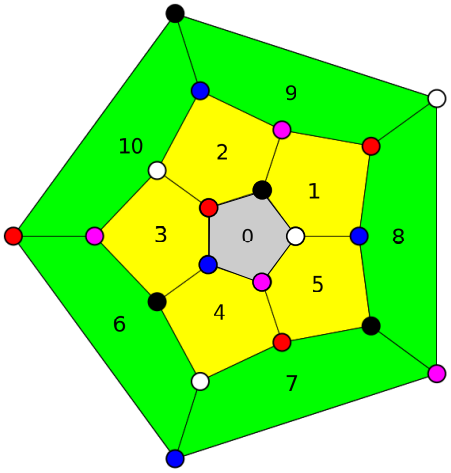

Figure 2.1: A diagram for the dodecahedron

Figure 2.1 also shows a particular 5-coloring of the vertices. This coloring has the property that the vertices of the same color are the vertices of a regular tetrahedron. This coloring will help us keep track of the orientations of the faces when we develop X out into the plane.

A geodesic segment in X cannot have any cone points in its interior. For this reason, any geodesic segment in X is transverse to the edges of X unless it lies in a single edge of X. We call such a geodesic segment *transverse*. We ignore the geodesic segments which lie in a single edge of X because they never arise in connection with the farpoint map.

Let γ^* be a transverse geodesic segment whose initial endpoint lies in $\Pi = \Pi_0$. There is a line segment $\gamma \subset \boldsymbol{C}$, and an embedded union of pentagons

$$\Pi_{i_0}, ..., \Pi_{i_k}$$

each sharing a side with the next, such that γ^* and γ have the same length, and $\gamma \cap \Pi_0 = \gamma^* \cap \Pi_0$. To cut down on redundancies, we insist that $i_0 = 0$ and that otherwise the pentagon chain is as short as possible. If the endpoints of

γ lie in the interior of faces of X then the pentagon chain is unique. The only potential non-uniqueness arises when the initial endpoint of γ is a vertex of Π_0, and here our "shortest chain" condition picks out a chain uniquely in this case. We will discuss an example below.

This rolling process is commonly called the *developing map*, and γ is commonly called the *developing image* of γ^*. We call $\Pi_0, ..., \Pi_{i_k}$ a *pentagon chain* and we sometimes refer to it by its associated sequence $i_0, ..., i_k$. We call the far endpoint of q of γ the *terminal point*. Thus, γ is the segment connecting p to q, and the distance from p to q^* *along* γ^* equals $|p - q|$.

Figure 2.2 shows the 3 pentagon chains of length at most 3 which are associated to minimal geodesic segments on X connecting a point in Π_0 to a point on Π_4. The associated sequences are 04 and 034 and 054.

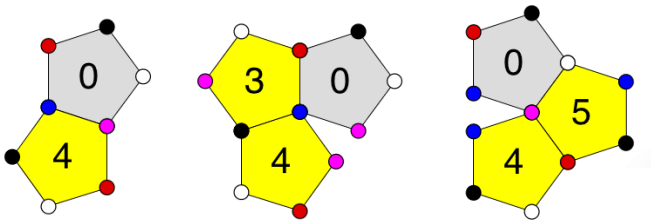

Figure 2.2: Chains connecting adjacent faces

The pentagon chains shown in Figure 2.3 do not arise in connection with a transverse geodesic segment. The only transverse segment the one on the left could be associated to starts at the red vertex of Π_0, but for such geodesic segments the chain does not have minimal length. The chain 034 above supports the same segments and is shorter than 0234. The chain on the right has a similar story. The only potential associated geodesic segments must end at the black vertex of X. The minimal chain in this case would be 036.

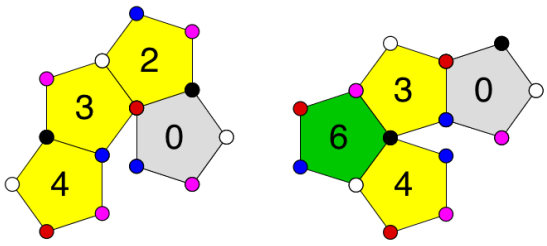

Figure 2.3: Two non-minimal chains

2.3 Crooked Chains

More generally, we define a pentagon chain to be any embedded chain of pentagons with the correct vertex colorings. The examples in Figure 2.3 are two such examples. We call such a pentagon chain *straight* if it contains a line segment with endpoints in the interiors of the initial and final faces. We call such a segment a *spanning segment*. We call a chain *crooked* if it has no spanning segment. The chains in Figure 2.3 are crooked. A chain arises in connection with a transverse geodesic segment on X if and only if it is straight.

One sure-fire way of generating straight chains is to draw geodesic segments on X, develop them out, and then see what chains we get. We do not like this method because it is hard to check that it is exhaustive. Our approach is to list out all possible chain sequences, from the tree of possibilities (up to a certain length), and then eliminate the crooked ones. Here we explain a computational criterion for crookedness.

Each pentagon chain defines a finite sequence of segments in the plane, namely the edges common to consecutive pentagons in the chain. We call a list of 3 edges *bad* if there is no line which intersects all three. If the pentagon chain contains a bad triple, then it is crooked. We can test computationally if a triple e_1, e_2, e_2 is bad in the following way. Let e_{k1} and e_{k2} be the endpoints of e_k. If e_{21} and e_{22} both lie on the same side of all 4 lines $\overline{e_{1i}e_{3j}}$ then the triple is bad.

If our test does not show that a chain is crooked it does not necessarily mean that the chain is straight. However, in practice, we can see immediately that all the remaining chains are indeed straight.

2.4 Mirror Images

We will generally be interested in pentagon chains whose sequences start with 0 and end in either 4, 9, or 11. (We make these choices somewhat arbitrarily.) To help us cut down on the enumeration, we note that the symmetry I of X which preserves the faces $\Pi_0, \Pi_4, \Pi_9, \Pi_{11}$ has the following action on chains:

$$(0,1,2,3,4,5,6,7,8,9,10,11) \leftrightarrow (0,2,1,5,4,3,7,6,10,9,8,11). \qquad (5)$$

What we mean is that the chains associated to the geodesics γ and $I(\gamma)$ are swapped by the symbolic map in Equation 5. This 034 and 035 are swapped. We call such pairs of swapped chains *mirror images*.

2.5 An Example Search

Here we use a computer search to prove a result which will be the basis for some other results we prove.

Lemma 2.2 *The only straight chains of the form* $0, ..., 4$ *associated to minimal geodesic segments are* 04 *and* 034 *and* 054.

Proof: An exhaustive computer search reveals that there are 8 straight pentagon chains of the form $0, ..., 4$ which have length $\ell \in \{4, 5, 6\}$. These are

$$0, 1, 8, 11, 6, 4, \quad 0, 1, 9, 10, 6, 4, \quad 0, 1, 9, 11, 6, 4 \quad 0, 1, 9, 11, 7, 4$$

and their mirror images. Figure 2.4 shows these chains.

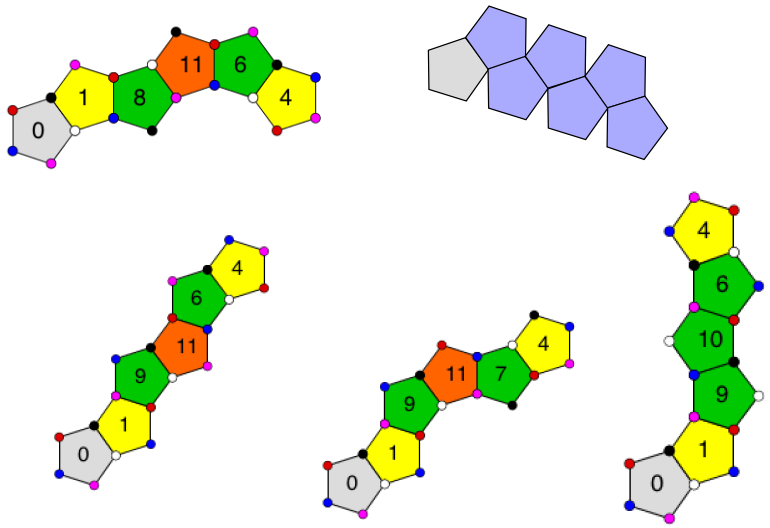

Figure 2.4: Two non-minimal chains

As we have already mentioned, every two points in Π_0 and Π_4 can be connected by a path of length at most $2 + \phi$. At the same time, no spanning segment for any of the chains in Figure 2.4 has length less than $2 + \phi$. Hence, none of the chains in Figure 2.4 corresponds to a minimal geodesic segment. The same goes for chains of length 7 or more, as one can see by considering the "tightest" case, shown in Figure 2.4, in which every three consective pentagons share a vertex. ♠

2.6 Voronoi Decompositions

Let $H \subset \boldsymbol{C}$ denote a convex polygon. We assume that no three vertices of H are collinear. Thus, H is convex in the strongest possible sense. We call H *strongly convex*. Let $p_1, ..., p_k$ be the vertices of H. Given $q \in H$, let

$$\mu_H(q) = \min_{j \in \{1,...,k\}} |q - p_j|. \tag{6}$$

We say that a *minimal index* for q is an index j such that $\mu_p(q) = |q - p_j|$. The jth *voronoi cell* for q is the set C_j of points having j as one of their minimal indices. That is, $\mu_p(q) = |q - p_j|$ if and only if $q \in C_j$. The list $C_1, ..., C_k$ is the *Voronoi decomposition* of H_p. The Voronoi cells are convex polygons. Each Voronoi cell has 2 edges in ∂H, and its remaining edges are contained in the union of visectors defined by pairs of vertices in H.

Let VH denote the Voronoi decomposition of H. We say that the *graph associated* to VH is the union of the boundarties of the Voronoi cells. This is a straight-line graph with finite valence. Here are a few more definitions we make in connection with this graph. We say that an *essential vertex* of VH is a vertex of some Voronoi cell that does not lie in ∂H. Each Voronoi cell has 3 vertices in ∂H, and its remaining vertices are essential.

We define a *triple point* to be a point that is equidistant from at least 3 vertices of H. We name triple points by the indices of 3 equidistant vertices. Every triple of indices gives rise to a triple point because H is strongly convex. All the essential vertices of VH are triple points but some triple points need not be essential vertices of VH. We also note that there might be several valid names for a triple point. For instance, if q is equidistant from p_1, p_2, p_3, p_4, then $(123), (124), (134), (234)$ are all valid names for q.

Often we will have a 2-parameter family $\{H_p\}$ of strongly convex polygons, which vary continuously depending on a parameter $p \in U \subset \boldsymbol{C}$. We call such a family *structurally stable* if all the vertices of VH_p have valence 3 and if the combinatorics of VH_p is independent of p. What this means is these vertices never coalesce as p varies in U. Put another way, structural stability means that none of the edges shrinks to a point as p varies.

We can test for structural stability computationally. An edge e_p of VH_p corresponds to a quadruple p_i, p_j, p_k, p_ℓ of vertices, all depending on p. If these vertices are never co-circular, then e_p never shrinks to a point. We can prove this by showing that the numerator of the imaginary part of the cross ratio of these points is nonzero on U. Thus we need a way to test that polynomials in domains are positive.

2.7 Positivity Certificates

Here I will describe a positivity certificate. There are many such certificates – e.g., Sturm sequences in one variable, sum-of-squares methods, the Handelman decomposition. As far as I know, I came up with the following one myself. It is quite easy to implement on a computer. I call it the *Positive Dominance Criterion*. See my monograph [**S2**] for details.

We consider the n-variable case. Define

$$x^I = x_1^{i_1}...x_n^{i_n}, \qquad I = (i_1, ..., i_n). \tag{7}$$

If $I' = (i_1', ..., i_n')$ we write $I' \leq I$ if $i_j' \leq i_j$ for all $j = 1, ..., n$. Consider a polynomial

$$F = \sum A_I X^I, \qquad A_I \in \boldsymbol{R}. \tag{8}$$

We call F *positive dominant* if

$$\sum_{I' \leq I} A_{I'} \geq 0 \qquad \forall I, \tag{9}$$

Lemma 2.3 *If F is positive dominant then $F \geq 0$ on $[0,1]^n$.*

Proof: We first prove this result in the 1-variable case. We suppose that $F(x) = a_0 + a_1 x + ... + a_n x^n$. The proof goes by induction on the degree. The case $\deg(F) = 0$ follows from the fact that $a_0 = A_0$. Let $t \in [0,1]$. We have

$$F(t) = a_0 + a_1 t + t_2 t^2 + \cdots + a_n t^n \geq a_0 t + a_1 t + a_2 t^2 + \cdots + a_n t^n =$$

$$t(A_1 + a_2 t + a_3 t^2 + \cdots a_n t^{n-1}) = tG(t) \geq 0$$

Here $G(t)$ is positive dominant and has degree $n-1$. In general,

$$F = f_0 + f_1 x_n + ... + f_m x_n^m, \qquad f_j \in \boldsymbol{R}[x_1, ..., x_{n-1}]. \tag{10}$$

Let $F_j = f_0 + ... + f_j$. Since F is positive dominant, we get that F_j is positive dominant for all j. By induction on n, we get $F_j \geq 0$ on $[0,1]^{n-1}$. But now, if we hold $x_1, ..., x_{n-1}$ fixed and let $t = x_n$ vary, the polynomial $g(t) = F(x_1, ..., x_{n-1}, t)$ is positive dominant.. Hence $g \geq 0$ on $[0,1]$. Hence $F \geq 0$ on $[0,1]^n$. ♠

Now let us restrict our attention to the 2-variable case. (Similar remarks apply in general, however.) Lemma 2.3 is the vanilla form of the criterion. Here we describe some augmentations and variants:

Subdivision: It might turn out that $F \geq 0$ on $[0,1]^2$ but that F is not positive dominant. Given some sub-rectangle $R \subset [0,1]^2$ we say that F is *induced positive dominant* on R if $F \circ \psi$ is positive dominant on $[0,1]^2$ for some choice of affine isomorphism $\psi : [0,1]^2 \to R$. In this case $F \geq 0$ on R. If we want to prove that $F \geq 0$ on $[0,1]^2$ and F is not positive dominant, we can check that F is induced positive dominant on $[0,1/2] \times [0,1]$ and $[1/2,1] \times [0,1]$. In practice this will mean checking that the functions $F_1(x,y) = F(x/2,y)$ and $F_2(x,y) = (1 - x/2, y)$ are both positive dominant. We could also subdivide in the Y-direction. Also, this trick can be iterated.

Triangular Domains: Sometimes we will want to know that $F \geq 0$ on a triangle Υ. To do this, we produce a polynomial map $\phi : [0,1]^2 \to \Upsilon$ and then consider the polynomial $F \circ \phi$ on $[0,1]^2$. Let T_0 be the triangle with vertices $(0,0)$, $(1,0)$ and $(1,1)$. The map ϕ is the composition $\phi_1 \circ \phi_2$ where ϕ_1 is an affine map from T_0 to Υ and $\phi_1(x,y) = (x,xy)$ is a map from $[0,1]^2$ to T_0. The map ϕ is a surjective polynomial map which induces a homeomorphism from $(0,1)^2$ to the interior Υ^o.

Strict Positivity: Sometimes we will want to check that $F > 0$ on $[0,1]^2$. If all the coefficient sums in Equation 9 are positive then we call F *strongly positive dominant*. The same argument as in Lemma 2.3 shows that $F > 0$ on $[0,1]^2$ when F is strongly positive dominant.

Even if F vanishes on some points on the boundary of $[0,1]^2$ we might want to know that $F > 0$ on $(0,1)^2$. Let F_Σ denote the sum of all the coefficients of F. We call F *solidly positive dominant* if F is positive dominant and $F_\Sigma > 0$. Essentially the same argument as in Lemma 2.3 shows that $F > 0$ on $(0,1)^2$ provided that F is solidly positive dominant.

We can combine these definitions with our subdivision approach. Suppose that we suspect $F > 0$ on $(0,1)^2$. If we can show that F_1 and F_2 above are both solidly positive dominant it means that $F > 0$ on $(0,1)^2$ except perhaps on the vertical segment $V = \{1/2\} \times (0,1)$. We then test the function $F_3(y) = F(1/2,y)$ and show that it is solidly positive dominant. This shows that $F > 0$ on V as well.

3 The Proof in Broad Strokes

3.1 The Antipodal Face

In §4 we will prove the following result.

Lemma 3.1 (Antipodal) *Given $p \in \Pi$, we have $\mathcal{F}_p \subset A(\Pi)$.*

This result involves a search through the tree of possible combinatorial types of length-minimizing segments on X. The analogous result for the octahedron is Statement 1 of [**S**, Octahedral Plan Lemma]. There the proof is easy because the regular octahedron develops out onto a global equilateral tiling of the plane.

Our proof of the Antipodal Lemma will reveal some additional structure of X: It will turn out that there are 70 pentagon chains associated to minimal geodesics starting in $\Pi = \Pi_0$ and ending in $A(\Pi) = \Pi_{11}$. Among these 70 chains, there are 10 of length 4, and the remaining 60 have length at least 5. Some computer experimentation reveals that each of these 70 chains does in fact arise in connection with some minimal geodesic segment.

3.2 Eliminating Combinatorial Types

We call a geodesic segment γ *straightforward* if it connects a point in Π to a point in $A(\Pi)$ and has an associated pentagon chain of length 4. A glance at Figure 3,1 below shows that any pair $(p, q) \in \Pi \times A(\Pi)$ has some straightforward geodesic segment connecting it.

It might be nice if we could simply say that for every $(p, q) \in \Pi \times A(\Pi)$ the distance $d_X(p, q)$ is realized by the length of a straightforward geodesic segment connecting them. Call this property S. Unfortunately property S can fail. What makes our proof of Theorem 1.2 work is that the failures of property S occur when q is far from $\mathcal{F}_p$. To formalize this idea, we define

$$\widehat{f}_X : \Pi \times A(\Pi) \to \boldsymbol{R} \tag{11}$$

as follows: $\widehat{d}_X(p, q)$ is the minimal length of all straightforward geodesic segments in X which join p to q. We are not claiming that $\widehat{d}_X$ is a metric, and the failure of property S tells us that sometimes $d_X < \widehat{d}_X$.

Still, we can use $\widehat{d}_X$ to define a "new" dynamical system by simply substituting $\widehat{d}_X$ for d_X in all the definitions of the farpoint map:

- $\widehat{\mathcal{F}}_p$ is the set of points in $A(\Pi)$ which maximize the function $\widehat{d}_X(p,*)$.
- We set $\widehat{F}(p)=q$ when $\widehat{\mathcal{F}}_p=\{q\}$.
- $\widehat{\mathcal{G}}_p=A(\widehat{\mathcal{F}}_p)$ and $\widehat{G}=A\circ\widehat{F}$.

In §4 we prove the following result:

Lemma 3.2 (Comparison) *Assume that $\widehat{\mathcal{G}}$ has the description given by Theorem 1.2. Then $\widehat{d}_X(p,\widehat{q})=d_X(p,\widehat{q})$ when $\widehat{q}\in\widehat{\mathcal{F}}_p$.*

The Comparison Lemma is the analogue of Statement 2 of [**S**, Octahedral Lemma], though the proof is different. Our proof here involves applying our positivity certificate to 360 different polynomials that arise when we compare $\widehat{d}_X$ and d_X.

Now we derive a corollary.

Corollary 3.3 *Assume that $\widehat{\mathcal{G}}$ has the description given by Theorem 1.2. Then $\mathcal{G}_p=\widehat{\mathcal{G}}_p$ for all $p\in\Pi$.*

Proof: Suppose that $p\in\Pi$ is such that $\mathcal{G}_p\neq\widehat{\mathcal{G}}_p$. Then $\mathcal{F}_p\neq\widehat{\mathcal{F}}_p$. Let $q\in\mathcal{F}_p$ and $\widehat{q}\in\widehat{\mathcal{F}}_p$. Since our sets mismatch, we can assume without loss of generality that either $q\notin\widehat{\mathcal{F}}_p$ or that $\widehat{q}\notin\mathcal{F}_p$.

In the first case we have

$$d_X(p,\widehat{q})\le d_X(p,q)\le\widehat{d}_X(p,q)<\widehat{d}_X(p,\widehat{q}).$$

In the second case, we have

$$d_X(p,\widehat{q})<d_X(p,q)\le\widehat{d}_X(p,q)\le\widehat{d}_X(p,\widehat{q}).$$

In both cases, this middle inequality comes from the fact that $d_X\le\widehat{d}_X$. Both these equations contradict the Comparison Lemma. ♠

In the rest of the chapter, we explain how we prove that $\widehat{\mathcal{G}}$ has the description given by Theorem 1.2. Then, at the end, we invoke Corollary 3.3 to conclude that Theorem 1.2 equally well describes $\mathcal{G}$.

3.3 The Decagon and the Hexagon

We first describe a coloring of X. We divide Π and $A(\Pi)$ into 5 triangles and color them so as to be invariant under A. We color the other 10 pentagons grey. This coloring is not so directly related to the vertex coloring discussed in connection with Figure 2.1, but nonetheless it is useful to us.

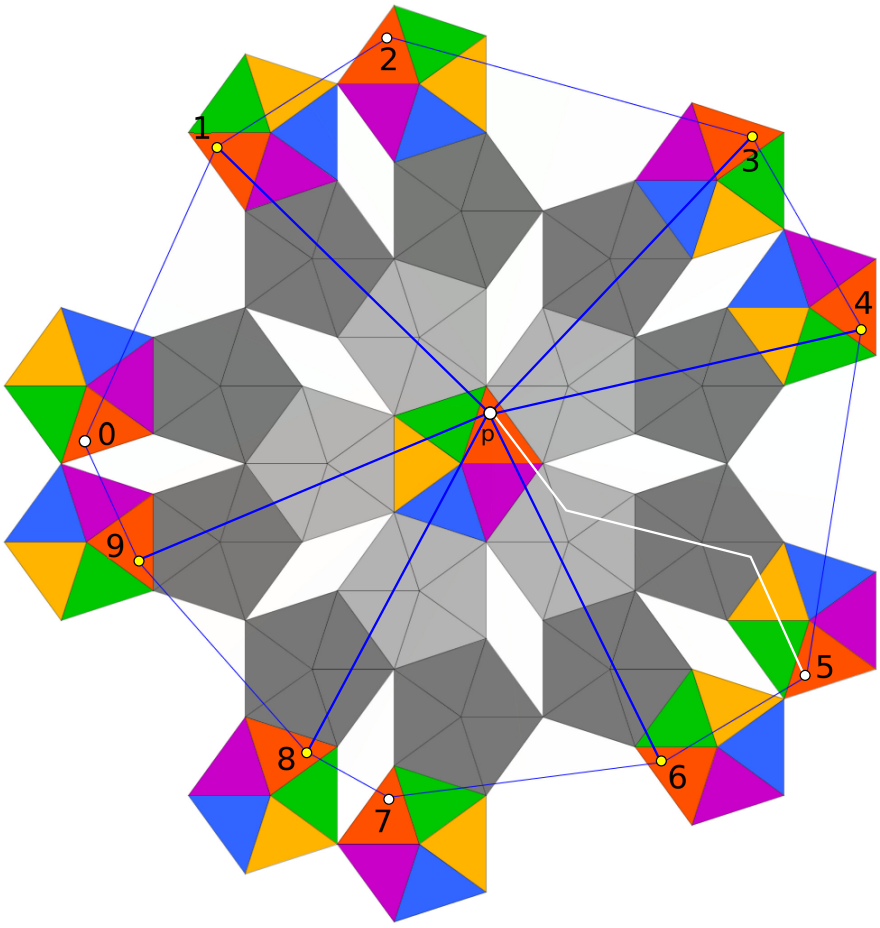

Figure 3.1: The dodecahedral plan.

Figure 3.1 shows the pentagon chains associated to the straightforward geodesics mentioned above. These chains have been superimposed over each other. Let P be the union of all these planar pentagons. The inner and outer pentagons are colored so as to be compatible with the developing map and with the coloring of X just described.

Let $P_{10} \subset P$ be the union of the outer 10 pentagons. There is a color-preserving 10-to-1 map $\Psi : P_{10} \to A(\Pi)$. The decagon D_p in Figure 3.1 has vertices

$$\Psi^{-1}(A(p)) = \{p_0, ..., p_9\}.$$

The number k in Figure 3.1 denotes p_k. By construction and by symmetry

$$\widehat{d}_X(p, A(q)) \geq \mu_{D_p}(q). \tag{12}$$

Here μ_{D_p} is as in Equation 6.

Remarks:
(i) The reason we could have strict inequality is that perhaps the line segment joining q to the closest vertex of D_p does not lie in P. In that case it would not correspond to a geodesic segment in X. The white zigzag in Figure 3.1 highlights an example where $\overline{pp_5}$ does not correspond to a geodesic segment in X.
(ii) We will not bother to prove that D_p is strongly convex, even though it is. Equation 6 makes sense even for non-convex polygons.
(iii) We mention one beautiful piece of structure. For each index i, we can consider the bisector β_i for the points (p_i, p_{i+5}), with indices taken mod 5. Thus β_i is the set of points equidistant from these two points. The 5 bisectors $\beta_0, \beta_1, \beta_2, \beta_4, \beta_5$ all cross at p and are parellel to the 10th roots of unity. They make a perfect asterisk at p. This does not just follow from symmetry: Rotation by $\pi/5$ about p is not generally a symmetry of D_p.

Let $\Delta \subset \Pi$ denote the central red triangle in Figure 3.1. This triangle has vertices $0, 1, \omega$, where $\omega = \exp(2\pi i/5)$. Let Δ_k be the outer red triangle labeled k in Figure 3.1. Looking at Figure 3.1 we can see the every point in Δ can be joined to every point of Δ_k for $k = 1, 3, 4, 6, 8, 9$ by a line segment that remains in P. Put another way when $p, q \in \Delta$ the segment $\overline{qp_k}$ lies in P for all $k = 1, 3, 4, 6, 8, 9$. This motivates us to define H_p denote the hexagon whose vertices are $p_1, p_3, p_4, p_6, p_8, p_9$. These are the vertices joined to p by line segments in Figure 3.1. Given the properties of H_p just mentioned, we have

$$\widehat{d}_X(p, A(q) = \widehat{d}_X(q, A(p)) \leq \mu_{H_p}(q) \tag{13}$$

Once again, we are referring to Equation 6.

Remarks:
(i) We might have inequality because the minimal geodesic joining p to $A(q)$ might develop out to a line segment connecting q to a vertex of D_p which is not a vertex of H_p.
(ii) Here is the proof that H_p is strongly convex for all $p \in \Delta$. Let A, B, C be three red triangles containing consecutive vertices of H_p. We can see directly that any line L that intersects both A and B separates all points of B from the origin. One just has to check the extreme cases where L goes through a vertex of A and a vertex of C.

We bothered to prove that H_p is strongly convex because we want to consider the Voronoi decomposition VH_p. We prove the following in §6.

Lemma 3.4 (Voronoi Structure) *Let $p \in \Delta$.*

1. *The essential vertices of H_p lie Δ.*
2. *If r is an essential vertex of H_p, then $\mu_{H_p}(r) = \mu_{D_p}(r)$.*

Figure 3.2 shows a typical picture of VH_p for $p \in \Delta$. The right side shows a closeup of the left side. The edge between the pink and purple cells is contained in the perfect asterisk remarked on above.

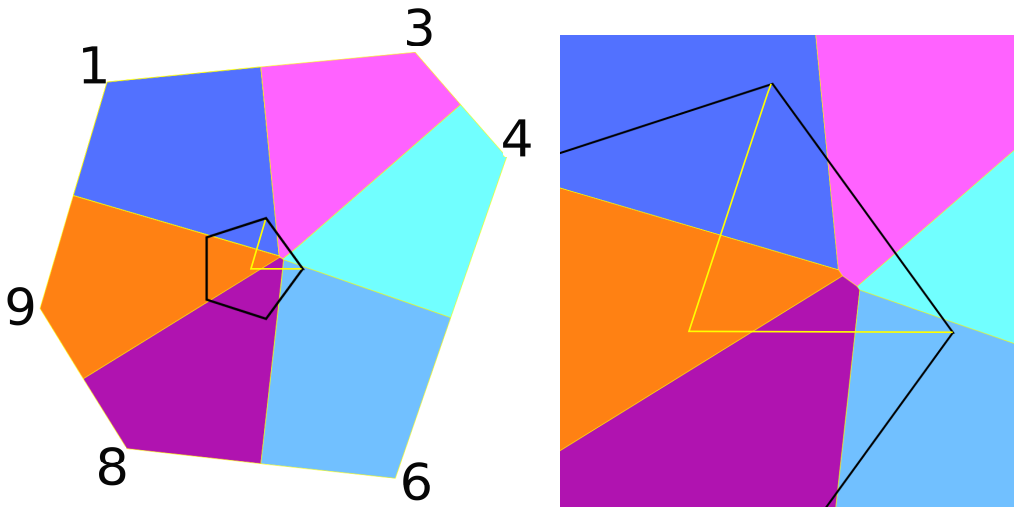

Figure 3.2: The Voronoi cell decomposition VD_p for typical p.

3.4 Setting up the Vertex Competition

By definition, $\widehat{\mathcal{G}}_p \in \Pi$ when $p \in \Pi$. In §6 we will deduce the following result from the Voronoi Structure Lemm:

Lemma 3.5 (Selection) *If $p \in \Delta$ then $\widehat{\mathcal{G}}_p \in \Delta$.*

Let D_p and H_p be the decagon and hexagon associated to $p \in \Delta$ as in the previous section. Recall that Π is the central pentagon. We have $\Delta \subset \Pi$.

Lemma 3.6 *The function μ_{H_p} takes its maximum exactly on some subcollection of the essential vertices of VH_p.*

Proof: Let $q \in H_p$ be some point, not necessarily in Δ. There is some Voronoi cell C_i such that $q \in C_i$. The function $f(q) = |q - p_i|^2$ is a convex function defined on C_i, and hence it is maximized exactly on some collection of the vertices of C_i. If $v = p_i$ then obviously f is not maximized at v. If $v \neq p_i$ is some inessential vertex of C_i then v is the endpoint of a bisector between C_i and $C_{i\pm 1}$. In this case, we increase $f(q)$ by pushing q along the bisector into H_p. This is to say that the vertices where f is maximized are essential vertices. But then $f(q) \leq f(r)$ for some essential vertex r, and the inequality is strict unless q is also an essential vertex. ♠

Our next result is closely related to [**R2**, Lemma 3] though it is stated in very different language.

Lemma 3.7 (Vertex) *If $q \in \widehat{\mathcal{G}}_p$, then q is an essential vertex of VH_p.*

Proof: Let μ_{H_p} By the Selection Lemma, we have $q \in \Delta$. We also have $\Delta \subset H_p$, by a wide margin. Hence $q \in H_p$. If q is not an essential vertex of VH_p then $\mu_{H_p}(p) < \mu_{H_p}(r)$ for some essential vertex r of VH_p. We have

$$\widehat{d}_X(p, A(q)) \leq \mu_{H_p}(p, q) < \mu_{H_p}(p, r) = \mu_{D_p}(p, r) \leq \widehat{d}_X(p, A(r). \tag{14}$$

The first inequality is Equation 13. The equality is the Statement 2 of the Voronoi Structure Lemma. The last inequality is Equation 12. The fact that $\widehat{d}_X(p, A(q)) < \widehat{d}_X(p, A(r))$ is a contradiction. ♠

3.5 The Vertex Competition

Figure 3.3 shows a close-up of the cities contained in the triangle Δ. There are 3 states contained in Δ, which we label $\Sigma_0, \Sigma_1, \Sigma_2$ as indicated. Let Υ_0 denote the half of Σ_0 lying beneath the dotted line. Our convention is that Υ_0 is closed, as is Σ_j for $j = 0, 1, 2$. In proving Theorem 1.2 it suffices by symmetry to take $p \in \Sigma_0 \cup \Sigma_1$. Henceforth we do this.

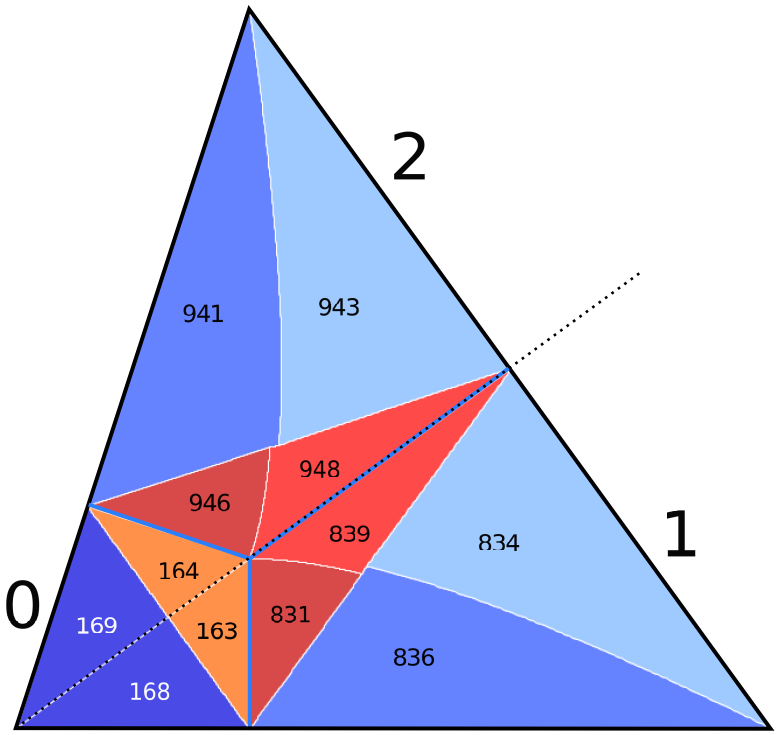

Figure 3.3: The cities in Δ.

Let (ijk, p) denote the unique point in H_p which is equidistant from the vertices p_i, p_j, p_k. This point may or may not be an essential vertex of VH_p, and perhaps there are other vertices of H_p that have the same distance to this point. From the Vertex Lemma, we know that every point of $\widehat{\mathcal{G}}_p$ has the form (ijk, p) for some triple of indices and moreover the point in question must be an essential vertex of VH_p. The rest of our proof just amounts to calculating which triple is assigned to which point. This boils down to algebra. In §7 we prove the following result.

Lemma 3.8 (Competition) *The following is true.*

1. *When $p \in \partial\Sigma_j$ for $j = 0, 1$ we have $\widehat{\mathcal{G}}_p = \{p\}$.*
2. *When $p \in \Upsilon_0^o$ we have $\widehat{\mathcal{G}}_p \subset \{(163, p), (168, p)\}$.*
3. *When $p \in \Sigma_0^o$ we have $\widehat{\mathcal{G}}_p \subset \{(163, p), (168, p), (164, p), (169, p)\}$.*
4. *When $p \in \Sigma_1^o$ we have $\widehat{\mathcal{G}}_p \subset \{(831, p), (834, p), (836, p), (839, p)\}$.*

Curiously, after all the algebra we do, this one result has an easy geometric proof.

Directly computing all these maps we see that whenever $\widehat{\mathcal{G}}_p$ is a singleton, the map $\widehat{G}$ is an $\mathcal{R}$-map adapted to Σ. Next, we identify the domains in Σ_0 and Σ_1 which correspond to each possible map and to verify that we have the combinatorial structure shown in Figure 1.4. This amounts explicit calculations involving polynomials. We carry this out in §7.

Given the Competition Lemma, the map $\widehat{G}$ from Theorem 1.2, when defined in terms of the function $\widehat{d}_X$, always has the form

$$\widehat{G}(p) = (ijk; p). \tag{15}$$

According to the Competition Lemma and symmetry there are 4 possibilities each within Σ_0 and Σ_1. When we explicitly compute all these maps, we find that the coincide with the $\mathcal{R}$-maps described in connection with Theorem 1.2. Now we apply symmetry to get similar results in all the states. All this shows that Theorem 1.2 really does describe $\widehat{\mathcal{G}}$.

Everything we have said so far concerns the map $\widehat{\mathcal{G}}$, which is defined in terms of our function $\widehat{d}_X$. But now we conclude from Corollary 3.3 that $\mathcal{G} = \widehat{\mathcal{G}}$. This completes the proof of Theorem 1.2.

4 The Antipodal Lemma

4.1 The Basic Chains

Let $p \in \Pi$ and $q^* \in \mathcal{F}_p$. In this chapter we prove that $q^* \in A(\Pi)$. We have already ruled out the case that q^* lies in a face of X adjacent to Π. By symmetry we just have to rule out the possibility that $q^* \in \Pi_9 - \Pi_{11}$. We argue by contradiction. We first consider the following 7 pentagon chains and their mirror images.

$$0,2,9 \quad 0,2,1,9 \quad 0,2,10,9 \quad 0,3,2,9 \quad 0,3,2,10,9$$

$$0,3,10,9 \quad 0,3,4,10,9. \tag{16}$$

We draw these pentagon chains in Figure 4.1. In each of the first 5 cases we add in the magenta line which goes through the magenta vertex of the the final pentagon and which is parallel to the opposite side of this pentagon. In the last 2 cases we draw not just this magenta line but also the parallel blue line which goes through the blue vertex of the final pentagon.

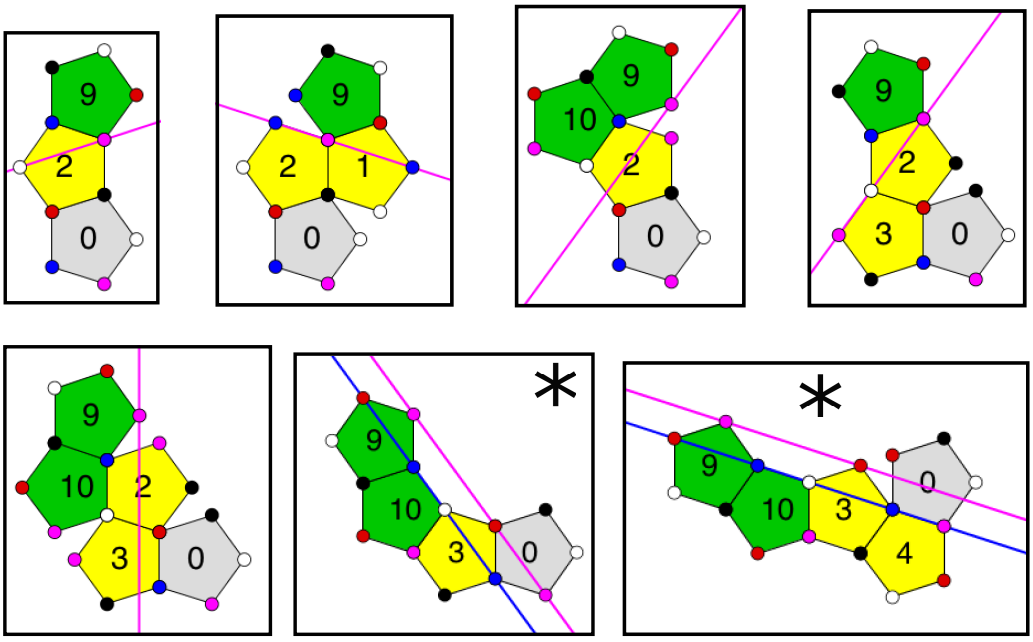

Figure 4.1: Seven basic pentagon chains

Below we will prove the following result.

Lemma 4.1 *The only chains of the form* $0, ..., 9$ *associated to minimal geodesic segments are the* 7 *basic ones and their mirror images.*

Lemma 4.2 *Lemma 4.1 implies the Antipodal Lemma.*

Proof: Consider the 5 cases which are not marked by $(*)$. Again, $q \in \boldsymbol{C}$ is the terminal point in the chain corresponding to $q^* \in X$. Let $r \in \boldsymbol{C}$ denote a point very near q which we reach by pushing q away from the magenta line and perpendicular to it. We call this the *magenta variation*. We have $|q-r| > |p-q|$ because the magenta line separates all points in the the final pentagon from all points in the initial pentagon, Π_0. In short, the magenta variation increases distances.

Consider the two remaining cases, the ones marked $(*)$. In these cases, the magenta variation may not increase distances, because the magenta line does not separate the final pentagon from Π_0. However, notice that in each of these cases, q cannot lie between the blue and magenta lines, because no line segment incident to such a point can connect to a point in Π_0 and yet remain in the pentagon chain. Hence q lies below the blue line. But then the blue line separates q from all of Π_0. So, once again, the magenta variation increases distances for all *relevant* choices of q.

By symmetry, the magenta variation also increases distances in the 7 mirror image chains.

Now consider all possible minimal geodesic segments connecing p to q^*. Even if there is more than one such, we can perform the magenta variation simultaneously with respect to all the pentagon chains. This gives rise to the same point $r^* \in X$ in all case. By compactness and Lemma 4.1, we can choose r^* close enough to q^* so that each minimal geodesic connecting p to r^* gives rise to one of the pentagon chains associated to minimal geodesics connecting p to q. But then each of these p-to-r^* geodesics is longer than the corresponding p-to-q^* minimal geodesics. In short, $d_X(p, r^*) > d_X(p, q)$. This proves that $q \notin \mathcal{F}_p$ under the assumption that Lemma 4.1 is true. ♠

The rest of the chapter is devoted to proving Lemma 4.1. The general idea of our proof of Lemma 4.1 is to take the other candidate pentagon chains, which we will discuss in the next section, and show in each case that they contain a certain quadrilatral Q which can be replaced by a "smaller" quadrilateral $\overline{Q}$ made from the edges of one of the $14 = 7+7$ pentagon chains discussed above. We first explain what we mean by this, and then we carry out the analysis.

4.2 Compressing Quadrilaterals

The edges of the pentagons in a pentagon chain have length $\ell = 2\sin(2\pi/5)$. We consider quadrilaterals $Q = (A_1, A_2, B_1, B_2)$ whose sides A_1A_2 and B_1B_2 have length ℓ. We call these sides *distinguished*. These quadrilaterals need not be embedded. Given a point $(u, v) \in [0,1]^2$ the segment $Q(u, v)$ is the one which connects the points

$$(1-u)A_1 + uA_2, \qquad (1-v)B_1 + vB_2.$$

The special segments $Q(0,0)$ and $Q(1,1)$ are the other edges of Q. The special segments $Q(0,1)$ and $Q(1,0)$ are the diagonals of Q. We denote the length of $Q(u, v)$ by $|Q(u, v)|$.

Given a second quadrilateral $\overline{Q}$ of the same form, we write $Q \geq \overline{Q}$ if $|Q(u, v)| \geq |\overline{Q}(u, v)|$ for all $u, v \in [0,1]^2$. We call $\overline{Q}$ a *compression* of Q in this case.

Lemma 4.3 *$Q \geq \overline{Q}$ provided that $|Q(i, j)| \geq |\overline{Q}(i, j)|$ for all $i, j \in \{0, 1\}$.*

Proof: The function $|Q(u, v)|$ is quadratic in u and v. Setting $v = 0$ and letting $u \to \infty$ we see that the coefficient of u^2 in this expression is ℓ^2. Likewise, the coefficient of v^2 in this expression is ℓ^2. Therefore

$$g(u, v) = |Q(u, v)| - |\overline{Q}(u, v)| = Au + Bv + Cuv, \tag{17}$$

for some constants A, B, C. The restriction of g to any horizontal line in $[0,1]^2$ is a linear function. Likewise the restriction of g to any vertical line in $[0,1]^2$ is a linear function. But a linear function on a segment which is non-negative at its endpoints is non-negative on the whole segment. Since $g(0,0), g(0,1) \geq 0$ we see that $g(0, v) \geq 0$ for all $v \in [0,1]$. Likewise $g(1, v) \geq 0$ for all $v \in [0,1]$. But now we restrict g to the line segment $v = v_0$. Since $g(0, v_0), g(1, v_0) \geq 0$ we see that $g(u, v_0) \geq 0$ as well. ♠

Each pentagon chain $C = (\Pi_0, ..., \Pi_{i_k})$ has a *bottleneck quadrilateral* Q whose distinguished sides are $\Pi_0 \cap \Pi_{i_1}$ and $\Pi_{i_{k-1}} \cap \Pi_9$. Our line segment which starts in Π_0 and ends in Π_9 must cross both edges Q. If we have a second pentagon chain $\overline{C}$ we say that the *comparison quadrilateral* is the quadrilateral $\overline{Q}$ having distinguished sides in the first and last pentagons with the same vertex colors as Q. The examples below will make thie definition more clear. See e.g. Figure 4.4. We call the second chain the *comparison chain*.

4.3 A Computer Search

We call a pentagon chain *inefficient* if its sequence $i_0, ..., i_k$ has the property that there is some index j such that $i_j \geq 6$ and $i_{j+1} \leq 5$. Otherwise we call the chain *efficient*.

Lemma 4.4 *A pentagon corresponding to a length-minimizing geodesic segment is efficient.*

Proof: pentagon chain corresponds to a length minimizing geodesic segment, then every initial portion of the chain does as well. Thus, using symmetry, we could find an inefficient chain of the form $0, ..., 4$ corresponding to a length minimizing geodesic segment. This contradicts Lemma 2.2. ♠

Now we describe the results of a 3-step computer search.

Step 1: We do a search over all efficient pentagon chains of length at most 8 which do not contain Π_{11}. We discover that all such pentagon chains of length 8 are bad and hence crooked. We retain the list of all non-bad pentagon chains and we check that each of these is straight. We call such pentagon chains *short*. We discard the 14 basic chains from above.

Step 2: From Step 1 we see that any straight pentagon which has no 11 in its sequence must have length at most 7. Now we do a search over all chains of length at most 9 whose sequence ends in $11, 9$. We retain the list of all non-bad pentagon chains, and we check that all these are straight. We call such pentagon chains *long*. From the remarks about Step 1, we know that we have found all efficient straight pentagon chains whose sequence ends in $11, 9$.

Step 3: We merge the list of short chains with the list of long chains. There are $38 = 2 \times 19$ chains on the list. We choose one representative from each pair of mirror chains. This leaves us with 19 *candidates*.

We will show that no candidate can be a associated to a distance minimizing segment in X connecting a point in Π_0 to a point in Π_9, and this result finishes the proof of Lemma 4.1. The reason is that any other straight chain is obtained from a candidate or its mirror by appending some pentagons. Any minimal geodesic giving rise to this even longer chain would have a sub-arc giving rise to a candidate or its mirror image.

4.4 The Isometric Cases

Figure 4.2 shows the first 3 candidates and the 3 basic chains which serve as comparison chains. Each candidate is on the left and the comparison chain is on the right. We have also drawn the bottleneck quadrilaterals on the left and the comparison quadrilaterals on the right. The comparison quads are not in the same orientation as the bottleneck quads, but each comparison quad is isometric to the corresponding bottleneck quad in a color-preserving way. This allows us to perform a length-decreasing surgery on any geodesic segment γ^* that give rise to the candidates. We will perform the surgery using the first candidate, and the operation works exactly the same way for the other two candidates.

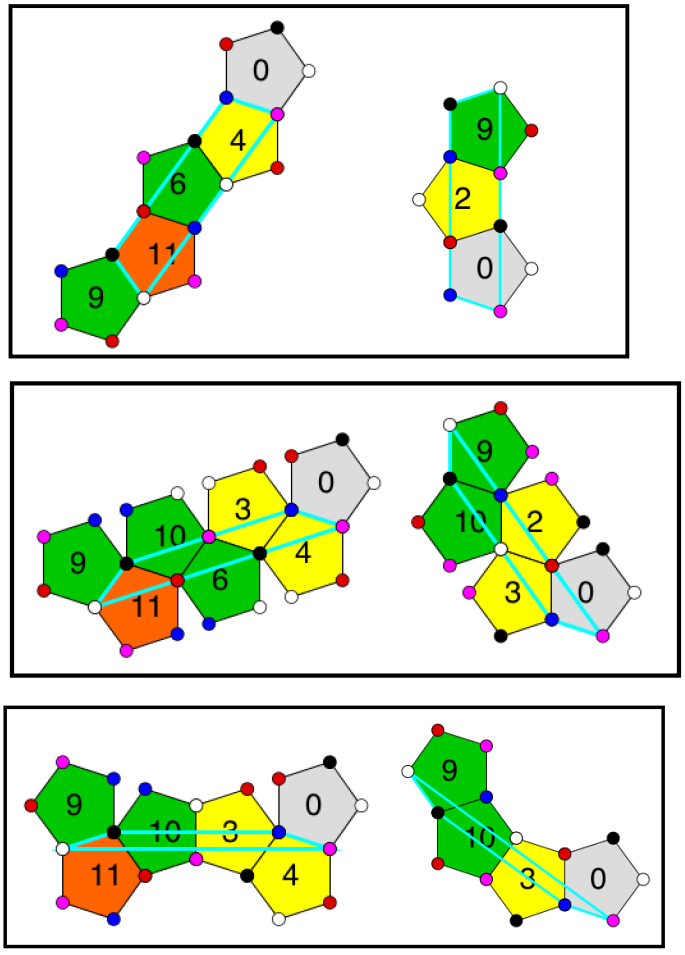

Figure 4.2: Three candidates and their comparison chains

Figure 4.3 illustrates our surgery operation. On the left we have the line segment $\gamma = \overline{pq}$ corresponding to γ^*. This segment goes through points p, d, c, b, a, q in order. The point a lies just a tiny bit inside Π_9, very near the the distinguished edge of Q. The points a, c are swapped by reflection in the cyan line through the distinguished edge of Q. Notice that the blue segment $\sigma'_L = \overline{cd}$ is shorter than the black segment $\sigma_L = \overline{ad}$.

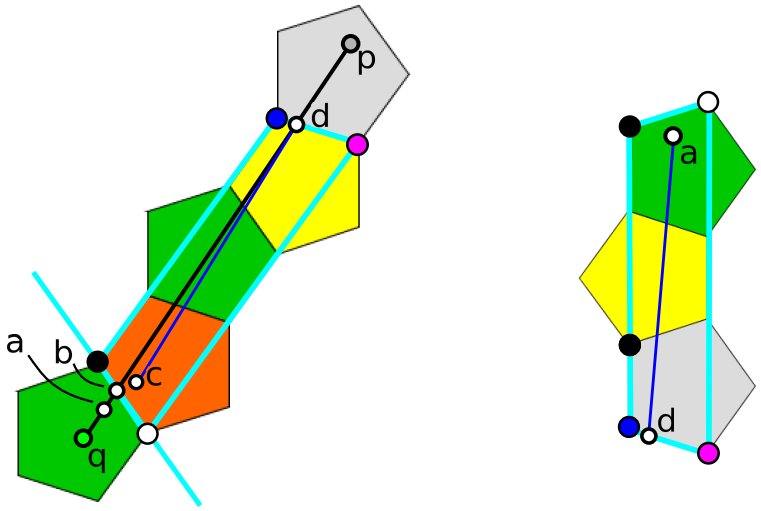

Figure 4.3: Three candidates and their comparison chains

On the right, the point a is in the same position in Π_9 as is the point a on the left. In other words, the points a^*_{left} and a^*_{right} in X corresponding to these points are the same point. Let a^* be this common point. Likewise, the d-point on the right is the same point as the d-point on the left. Let d^* be the corresponding point in X. We have $a^*, d^* \in \gamma^*$. By construction, the blue segment $\sigma_R = \overline{ad}$ on the right is isometric to the blue segment $\sigma'_L = \overline{cd}$ on the left. Hence σ_R is shorter than σ_L. But the corresponding segments σ^*_L and σ^*_R have the same endpoints in X, namely a^* and d^*. Hence, if we cut out σ^*_L from γ^* and replace it with σ^*_R we have a shorter polygonal path with the same endpoints as γ^*. This shows that γ^* is not a minimal geodesic segment.

One final word: The only way this argument could fail is if we have no choice of a which places c inside Q. This happens only if γ lies the line

extending the edge of Q having white and pink vertices. But then γ^* contains a cone point in its interior and is not distance minimizing.

Now we move on to more candidates. Figure 4.4 shows 3 more candidates on the left and the basic comparison chains on the right.

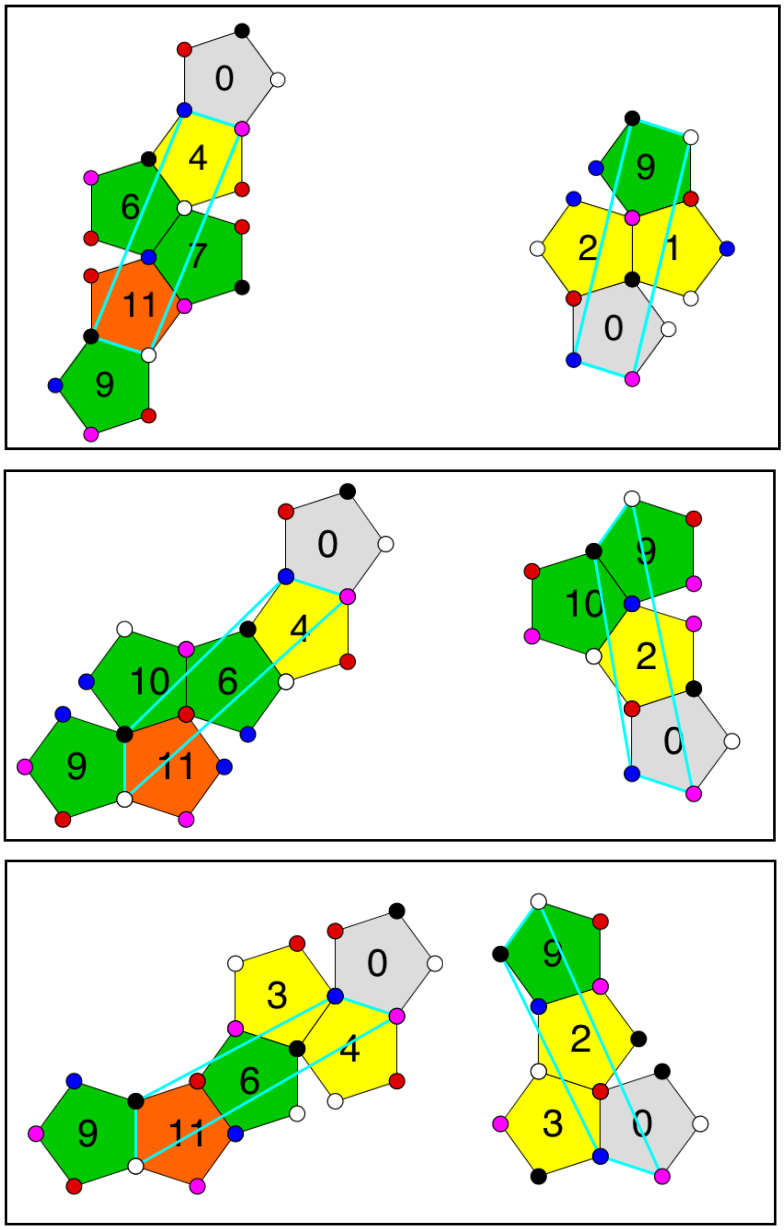

Figure 4.4: Three candidates and their comparison chains

As in the previous case, the bottleneck quads and the corresponding comparison quads are isometric in a vertex-color-preserving way. The difference here is that not every segment connecting the distinguished edges in the comparison quad lies inside the pentagon chain. Thus, we might have trouble drawing the blue segment $\sigma_R = \overline{ad}$ on the right in Figure 4.3. Let us look at this closely. Say that a *spanning segment* in the bottleneck quad is one which has its endpoints in the distinguished segments of the quad. Call a spenning segment in the bottleneck quad *realizable* if it lies in the pentagon chain. Make the same definitions for the comparison quad.

A close look at the pictures (or a computer plot, as we did) reveals that the vertex-color-preserving isometry from the bottleneck quad to the comparison quad maps realizable spanning segments to realizable spanning segments. Referring to Figure 4.3, the spanning segment $\overline{bd}$ on the left is realizable. Hence, by compactness, the segment $\overline{cd}$ lies in the comparison chain provided that we choose a sufficiently close to b. The only way this could fail is if $\gamma = \overline{pq}$ contains a vertex of the chain. But in this case, γ^* contains a cone point in its interior. So, once again, we can shorten γ^* by surgery.

4.5 Compressing Cases

For the next group of candidates, the bottleneck quadrilateral Q is not isometric to the comparison quadrilateral $\overline{Q}$. However, two nice things are true.

1. We have $Q \geq \overline{Q}$. We test this using the criterion in Lemma 4.3.

2. Every spanning segment of the comparison quad $\overline{Q}$ is realizable.

Even though Q and $\overline{Q}$ are not isometric, there is a canonical correspondence between spanning segments with respect to Q and spanning segments with respect to $\overline{Q}$. Corresponding segments cut the distinguished edges at the same places – i.e., they correspond to the same point in the unit square from §4.2. This correspondence lets compare the segments σ_L' and σ_R which arise in the surgery.

Referring to the surgery in Figure 4.3, $\sigma_R = \overline{ab}$ on the right might not be isometric to $\sigma_L' = \overline{dc}$ on the left. However, the inequality $Q \geq \overline{Q}$ in each case quarantees that σ_R is not longer than σ_L'. So, again, σ_R is shorter than σ_L and we may do our surgery operation successfully.

Figure 4.5 shows each of the candidates in this group, and their comparison basic chains. The reader can see bigger pictures using our program.

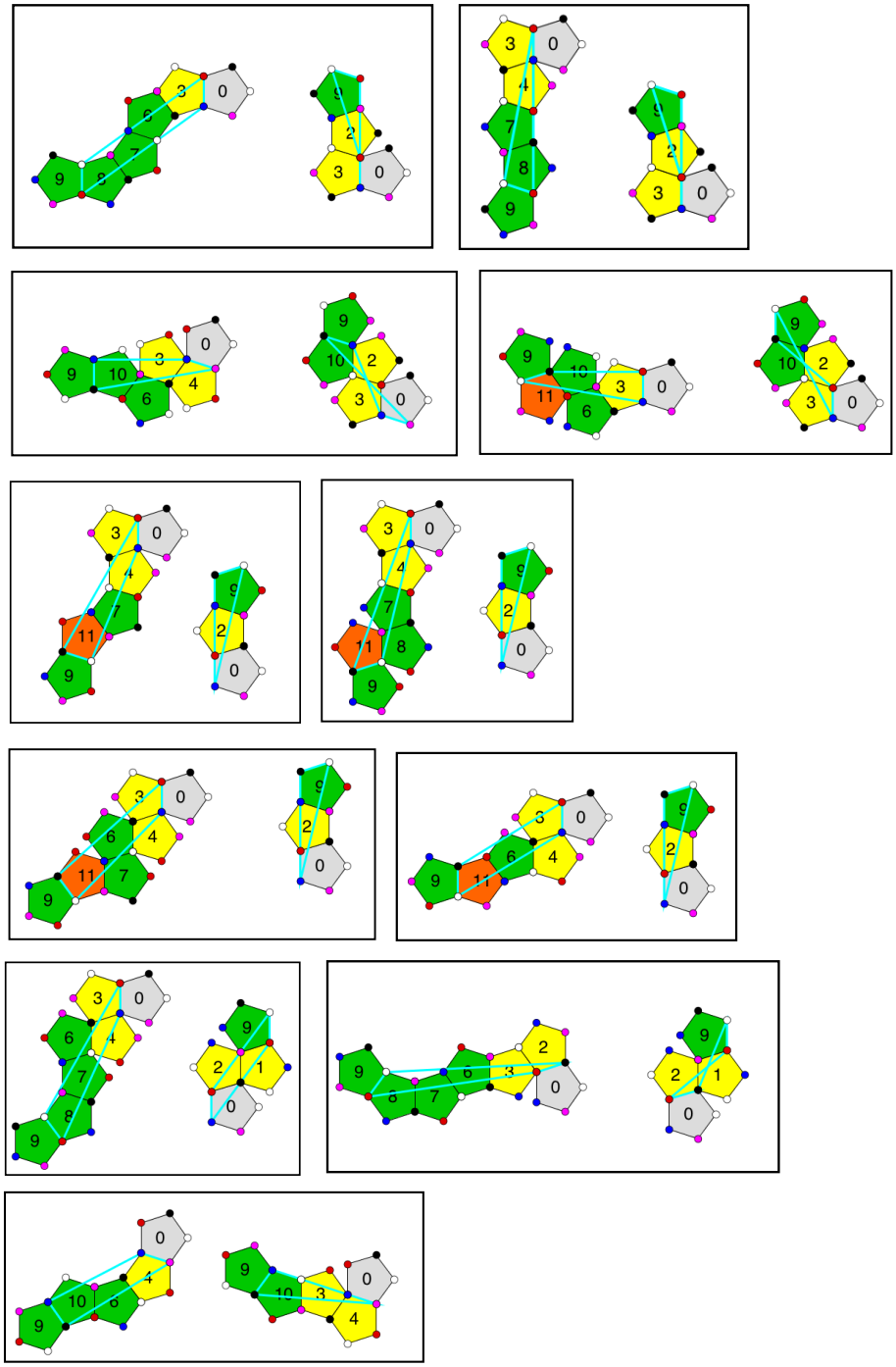

Figure 4.5: The candidates with compressing bottlenecks

Figure 4.6 shows the next case, which is more subtle than the ones above. We still have $Q \geq \overline{Q}$. This time not all spanning segment in $\overline{Q}$ are realized.

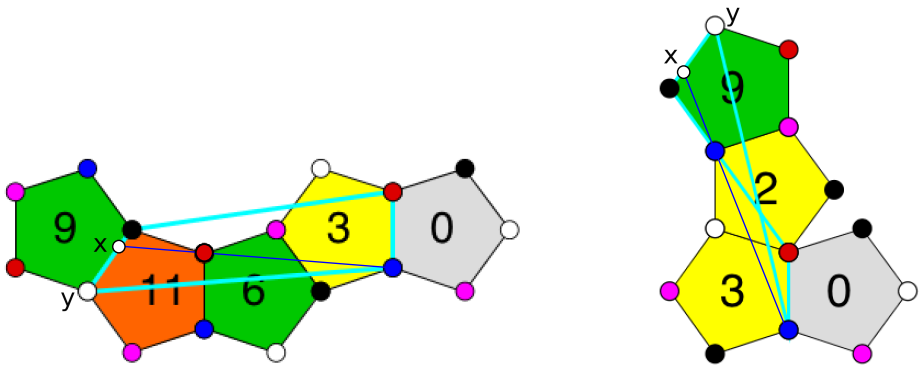

Figure 4.6: A subtle compressing case

Here is the fact that makes this case work: If s is a spanning segment with respect to Q that is realizable then the corresponding segment with $\overline{s}$ is realizable with respect to $\overline{Q}$. To see this, note that the point x in both figures lies in the same position with respect to the distinguished segment that contains it. Any realizable spanning segment with respect to Q must have an endpoint in $\overline{xy}$. At the same time, every spanning segment with respect to $\overline{Q}$ having an endpoint in $\overline{xy}$ is realizable. That is, having an endpoint in $\overline{xy}$ is necessary for spanning on the left, and sufficient for spanning on the right. Given this property of spanning segments, the surgery operation works just as it does for the other cases with a compressing bottleneck.

4.6 One Final Case

The final case is the trickiest one. Figure 4.7 shows the final candidate and a comparison chain for which $Q \geq \overline{Q}$. Unfortunately, our luck runs out. All spanning segments with respect to Q are realized, but some spanning segments with respect to $\overline{Q}$ are not realized. This means that we cannot always do our surgery. We need to scramble to get this case to work.

Let us choose our colors so that the coordinates on $[0,1]^2$, corresponding to spanning segments, have the following meaning.

- $(0,0)$ is the segment joining the red vertex to the white vertex.
- $(1,0)$ is the segment joining the blue vertex to the white vertex.

- $(0,1)$ is the segment joining the red vertex to the black vertex.
- $(1,1)$ is the segment joining the blue vertex to the black vertex.

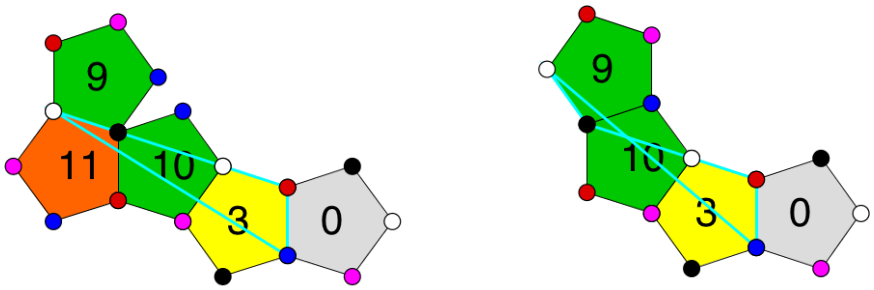

Figure 4.7: A compressing case that does not always work

Notice that the spanning segment $\overline{Q}(0,0)$ is not realizable but $\overline{Q}(1,0)$ and $\overline{Q}(0,1)$ and $\overline{Q}(1,1)$ are all realizable. A calculation shows that $\overline{Q}(u,v)$ is realizable provided that $u+v \geq 1$. This means that we can apply our surgery whenever the intersection with the segment $\gamma = \overline{pq}$ with Q is a segment of the form $Q(u,v)$ with $u+v \geq 1$.

Figure 4.8 shows another comparison chain. In this case, the two comparison quads are isometric, but the isometry does not preserve the colors. A calculation shows that $\overline{Q}(u,v)$ is not longer than $Q(u,v)$ provided that $u+v \leq 1$. Furthermore, every spanning segment with respect to $\overline{Q}$ is realizable. It is not true that $Q \geq \overline{Q}$. So, if our segment γ intersects Q in a segment of the form $Q(u,v)$ with $u+v \leq 1$ we can apply our surgery. So, in all cases, we can perform the surgery and shorten γ.

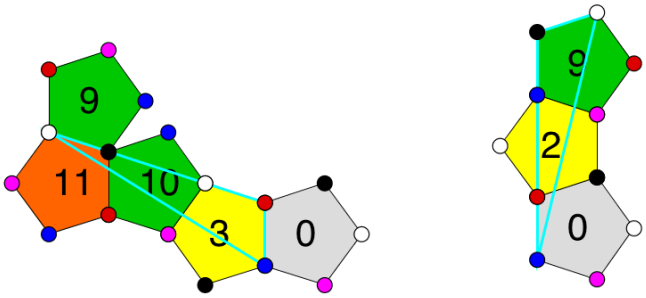

Figure 4.8: A partially compressing case

5 The Comparison Lemma

5.1 Confining the Cities

Our goal in this chapter is to prove the Comparison Lemma. It is important to mention the logical structure of our argument. Even though, at this point in the paper, we have not yet proved Theorem 1.2, we nonetheless can study properties of the maps defined in Theorem 1.2. As we have already discussed, one hypothesis of the Comparison Lemma is that the description in Theorem 1.2 really does describe the map $p \to \widehat{\mathcal{G}}_p$, the map defined in terms of our function $\widehat{d}_X$.

We denote cities by their corresponding triple points. Thus in C_{834}, the map G is given by $G(p) = (834; p)$. This is the point equidistant from the vertices p_8, p_3, p_4 of the decagon D_p. Our ordering of the points is such that the first two digits are common to all 4 cities within a state.

Now we discuss the relevant states. Let Σ_0 be the state containing the cities

$$C_{163}, C_{168}, C_{164}, C_{169}.$$

Let Υ_0 denote the bottom half of Σ_0, namely the union of C_{163} and C_{168}. Let Σ_1 be the state containing the cities

$$C_{831}, C_{834}, C_{836}, C_{839}.$$

Figure 5.1 shows the these cities, and also some auxiliary line segments.

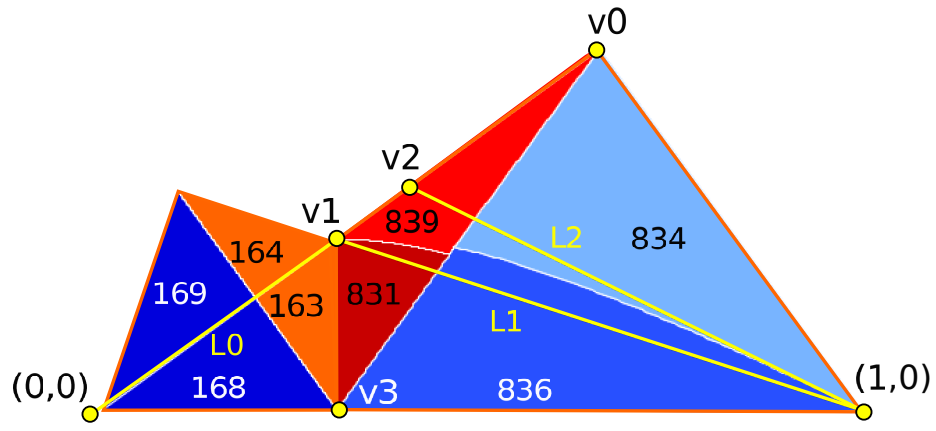

Figure 5.1: The cities contained in states Σ_0 and Σ_1.

It suffices to prove the Comparison Lemma when $p \in \Upsilon_0 \cup \Sigma_1$. The cities are curvilinear regions within their states, and for the purposes of computation we would prefer to deal with entirely polygonal (and in fact triangular) domains. In this section we set this up. Figure 5.1 also shows 3 vertices with the following coordinates:

$$v_0 = \frac{\phi \exp(\pi i/5)}{2}, \qquad v_1 = \frac{\exp(\pi i/5)}{\phi^2}, \qquad v_2 = \frac{\exp(\pi i/5)}{2}. \tag{18}$$

We define the following 3 triangles:

- Υ_{1638} is the right triangle with vertices $(0,0)$, v_3, and v_1.
- Υ_{8349} is the triangle whose vertices are $(1,0)$, v_0, and v_1.
- Υ_{8316} is the triangle whose vertices are $(0,0)$, $(1,0)$ and v_2.

By symmetry we have

Lemma 5.1 (Confinement) *We have*

- $C_{163} \cup C_{168} \subset \Upsilon_{1638}$.
- $C_{834} \cup C_{839} \subset \Upsilon_{8349}$.
- $C_{831} \cup C_{836} \subset \Upsilon_{8316}$.

Proof: The first of these results follows from symmetry. For the other statements, define

$$f_{ijk\ell} = |(ijk, p) - p_i|^2 - |(ij\ell, p) - p_i|^2, \tag{19}$$

We check that the functions f_{8346} and f_{8319} respectively do not vanish on L_1 and L_2, except at the endpoints. We then check that the signs are correct. For instance, $f_{8319} > 0$ on C_{831}, and we check that $f_{8319} > 0$ on the interior of L_1 and $f_{8319} < 0$ on the interior of L_2. Since the description in Theorem 1.2 gives these cities as connected sets, we see that the facts just established prove our claims. ♠

We note that $C_{163}, C_{168} \subset \Upsilon_{8316}$ as well, but Υ_{1638} gives a tighter fit.

5.2 The Proof

Given the analysis in the previous chapter, the only pentagon chains corresponding to minimal geodesic segments joining p to some point of $A(\Pi)$ are obtained from appending an 11 to each of the basic chain sequences shown in Figure 4.1 or else taking the dihedral image of such a chain. This gives us a collection of 70 *admissible chains*. Of the 70 admissible chains, 10 have length 4. These correspond to the straightforward geodesic segments. We call these 10 chains *straightforward*. Let $\mathcal{S}$ denote the collection of 10 straightforward chains. Let $\mathcal{B}$ denote the collection of the 60 other chains.

As usual we take $p \in \Sigma_0 \cup \Sigma_1$. For concreteness we will describe our proof for $p \in C_{834}$. We treat the other 5 cities exactly the same way. For $p \in C_{834}$ we have

$$\widehat{d}_X(p, \widehat{G}(p)) = |(834;p) - p_8| = |(834;p) - p_3| = |(834;p) - p_4|. \tag{20}$$

The point $(834;p)$ is equidistant from the 3 points p_8, p_3, p_4. The 3 points p_3, p_4, p_8 are three of the vertices of the decagon in Figure 3.1. We give formulas in §8.1. At the same time, there are 60 points $q_k = \langle C_k, p \rangle$ corresponding to each of the 60 chains $C_1, ..., C_{60} \in \mathcal{B}$. Again, we give formulas in §8.1. To show that

$$\widehat{d}_X((834;p), p) = d_X((834;p), p)$$

it suffices to show that

$$|(834;p) - p_j| \le |(834;p) - r_k| \qquad \forall j \in \{8,3,4\}, \qquad \forall k \in \{1, ..., 60\}. \tag{21}$$

We use a trick to avoid computing the triple points. We consider the polynomials

$$P_k = \Im \frac{(p_8 - p_4)(p_3 - r_k)}{(p_8 - p_3)(p_4 - r_k)}, \qquad k = 1, ..., 60. \tag{22}$$

Here we are taking the imaginary part of the cross ratio. The function P_k is a rational function of (x, y), and positive when p_k lies outside the disk bounded by the circle containing p_8, p_3, p_4. Also $P_k = 0$ if and only if the points are co-circular. So, it suffices to show $P_k \ge 0$ on Υ_{8346} for all $k = 1, ..., 60$. We complete the proof by doing this. We do all the same steps for the remaining five city-triangle pairs (C, Υ) with $C \subset \Upsilon$.

To analyze the 360 functions of interest to us, we use the techniques described in §2.7. In §8.2 we give formulas for surjective polynomial maps

from $[0,1]^2$ to each triangle Υ mentioned above. For each relevant rational function P_k and each relevant triangle map F we consider

$$Q_k = \text{numerator}(P_k \circ F). \tag{23}$$

We choose the numerator so that the sum of all the coefficients of Q_k is positive. That is, $Q_k(1,1) > 0$.

By construction $P_k \geq 0$ on Υ_{8349} if and only if $Q_k \geq 0$ on $[0,1]^2$. Each polynomial Q_k has the form

$$Q_k(x,y) = \sum_{i,j \leq 3} c_{ijk} x^i y^j, \qquad c_{ijk} \in \boldsymbol{Q}(\sqrt{2}, \sqrt{5}, \sqrt{5-\sqrt{5}}, \sqrt{5+\sqrt{5}}). \tag{24}$$

In all 360 cases, we check that both polynomials

$$Q_1(x,y) = Q(x/2, y), \qquad Q_2(x,y) = (1 - x/2, y)$$

are positive dominant. This completes the proof.

6 The Voronoi Decomposition

In this chapter we prove the Voronoi Structure Lemma. At the end of the chapter we deduce the Selection Lemma from the Voronoi Structure Lemma.

6.1 Four Triangles

The Voronoi Structure Lemma makes two statements about the structure of VH_p, the Voronoi decomposition of the hexagon H_p. By symmetry it suffices to take our point p in the union $\Upsilon_0 \cup \Sigma_1$ discussed in the last chapter. In the previous chapter we covered Σ_1 with two other triangles. In this chapter we make a sharper partition. We write $\Sigma_1 = \Upsilon_1 \cup \Upsilon_2 \cup \Upsilon_3$ where

1. Υ_1 is the triangle with vertices v_1, v_3 and $(1,0)$.
2. Υ_2 is the triangle with vertices v_1, v_2 and $(1,0)$.
3. Υ_3 is the triangle with vertices v_0, v_2 and $(1,0)$.

Figure 6.1 shows these 4 triangles.

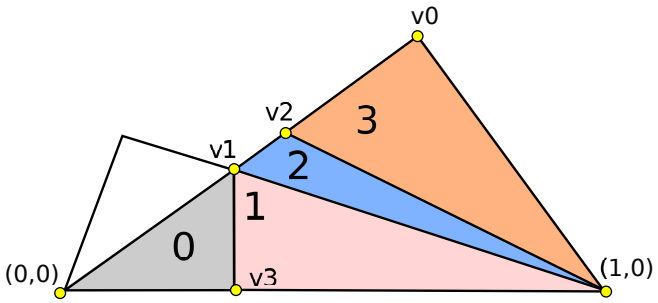

Figure 6.1: The 4 triangles Υ_j for $j = 0, 1, 2, 3$.

In §8.2 we describe polynomial maps $F_j : [0,1]^2 \to \Upsilon_j$ for $j = 0, 1, 2, 3$. These maps play an important role in our proof, just as similar maps played an important role in the previous chapter. We note that F_j gives a homeomorphism between $(0,1)^2$ and the interior of Υ_j.

6.2 A Special Edge

The vertices of the hexagon H_p are $p_1, p_3, p_4, p_6, p_8, p_9$. We give formulas in §8.1. A direct calculation shows that

$$|p - p_j| = |p - p_{j+5}|, \qquad j = 1, 3. \tag{25}$$

Thus p lies in the bisectors b_{16} and b_{38}.

Remark: We called these two bisectors β_1 and β_3 in Remark (iii) after Equation 12. Equation 25, which holds for all $j = 0, 1, 2, 3, 4$, is partly responsible for "asterisk" mentioned in Remark (iii).

Lemma 6.1 *If $p \in \Upsilon_0^o$ then VH_p has an edge e_{16} which contains p in its interior and is contained in b_{16}.*

Proof: This result follows from the claim that

$$\Phi_j = |p - p_j|^2 - |p - p_1|^2, \qquad j = 3, 4, 8, 9. \tag{26}$$

is positive on Υ_0^o, because then p will lie only in the Voronoi cells C_1 and C_6 and e_{16} is the intersection of these cells. Let $G_j = \Phi_j \circ F_0$, where F_0 is our triangle map. For each $j = 3, 4, 8, 9$ we show that the functions

$$G_j(x/2, y), \quad G_j(1 - x/2, y), \quad G_j(1/2, y)$$

are solidly positive dominant. But then $G_j > 0$ on $(0, 1)^2$. But then $F_j > 0$ on Υ_o^o, as claimed. ♠

Lemma 6.2 *If $p \in \Sigma_1^o$ then VH_p has an edge e_{38} which contains p in its interior and is contained in b_{38}.*

Proof: The proof is similar to the proof in the previous case, but somewhat more involved. This result folllows from the claim that

$$\Phi_j = |p - p_j|^2 - |p - p_2|^2, \qquad j = 1, 4, 6, 9. \tag{27}$$

is positive on Σ_1^o.

Using the same technique as in the previous case we establish that each Φ_j is positive on Υ_k^o for $k = 1, 2, 3$. It remains to deal with the two lines $L_1 = \Upsilon_1 \cap \Upsilon_2$ and $L_2 = \Upsilon_2 \cap \Upsilon_3$. Under the maps F_1 and F_2, the points $(x, 1)$ correspond to points on L_1 and L_2 respectively. We set $y = 1$ and observe that the resulting functions $x \to \Phi_j \circ F_k(x, 1)$ are strongly positive dominant for all relevant indices. This shows that F_j is also positive on the relative interior of L_1 and L_2. Now we have covered all points of Σ_0^o. ♠

The existence of e_{16} places strong restrictions on what VH_p can look like when $p \in \Upsilon_0^o$. Figure 6.1 shows 3 of the 9 possible combinatorial types for $p \in \Upsilon_0^o$. These 3 cases will give a strong suggestion as to what the other 6 possibilities are. Note that we are just giving a combinatorial representation, and not a geometric one. The white dot represents p.

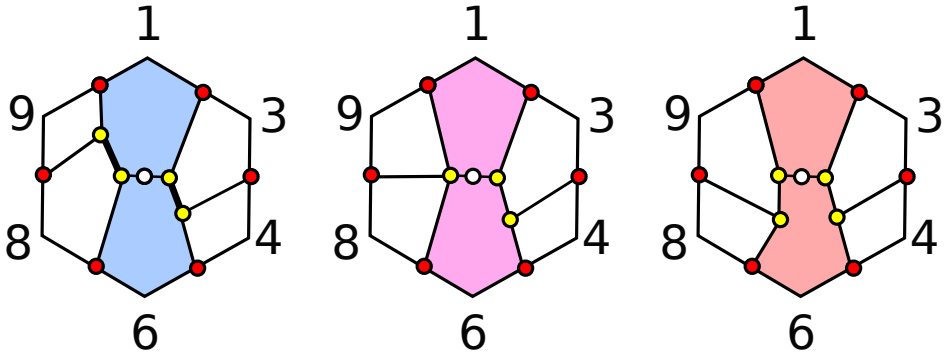

Figure 6.1: 3 of 9 combinatorial types for $p \in \Upsilon_0$.

The picture for $p \in \Sigma_1^o$ is similar, except that the indices $(1, 3, 4, 6, 8, 9)$ are replaced by the indices $(3, 4, 6, 8, 9, 1)$. That is, we just rotate the indices by one click.

Notice that the structure we have just established places some restrictions on the vertices of VH_p. For instance, when $p \in \Upsilon_0^o$ the vertices must lie in the set:

$$\{(168; p),\ (189; p),\ (689; p),\ (169; p),\ (134; p),\ (146; p),\ (346; p),\ (136; p)\}.$$

By continuity the same holds when $p \in \partial\Upsilon_0$. One can view our result about the special edge as establishing partial structural stability for H_p in the sense of §2.6. In the next section we take this further.

6.3 Structural Stability

Now we use our computational method to establish some of the structural stability we mentioned in §2.6. We first observe that VH_p is not structurally stable in the small triangle Υ_2. This triangle contains the interfaces between the cities C_{834} and C_{836} for instance. We have designed our partition of Σ_1 to concentrate all the instability into this one small triangle.

Lemma 6.3 *VH_p is structurally stable for $p \in \Upsilon_0^o$.*

Proof: We consider the cases in turn. We first check for some $p \in \Upsilon_0^o$ that the graph for VH_p is isomorphic to the left one in Figure 6.1. Since the edge e_{16} exists relative to all $p \in \Upsilon_0^o$ it suffices to show that the thick edges in Figure 6.1 never shrink to points as p varies in Υ_0^o. These edges correspond to the quadruples $\{1,6,8,9\}$ and $\{1,3,4,6\}$. For each quadruple (i,j,k,ℓ) let $P(i,j,k,l,x,y)$ denote the imaginary part of the cross ratio of p_i, p_j, p_k, p_ℓ as a function of $p = x + iy$. This is just as in Equation 22. We let Q denote the numerator of $P \circ F_0$, where F_0 is the triangle map to Υ_0. For both choices of Q we check that the two functions $Q(x, y/2)$ and $Q(x, 1-y/2)$ are solidly positive dominant. We also check that $Q(x, 1/2)$ is solidly positive dominant. This proves that $Q > 0$ on $(0,1)^2$. Hence $P > 0$ on Υ_0^o.

Lemma 6.4 *VH_p is structurally stable for $p \in \Upsilon_1^o$ and for $p \in \Upsilon_3^o$.*

Proof: The proof is similar to what we did in the previous case. This time (in both cases) the two edges of interest to us correspond to the quadruples $\{1,3,8,9\}$ and $\{3,4,6,8\}$ and the triangle maps are F_1 and F_3. Let Q be the polynomial that arises in each of the 4 cases, as in the previous lemma. We check that the 4 functions

$$Q(x/2, y/2),\ Q(x/2, 1-y/2),\ Q(1-x/2, y/2),\ Q(1-x/2, 1-y/2)$$

are solidly positive dominant. This shows that $Q > 0$ on $(0,1)^2$ except perhaps on the segment $\{1/2\} \times (0,1)$ and $(0,1) \times \{1/2\}$. We then show that the 4 single variable polynomials

$$Q(1/2, y/2),\ Q(1/2, 1-y/2),\ Q(x/2, 1/2),\ Q(1-x/2, 1/22)$$

are solidly positive dominant, and we check explicitly that $Q(1/2, 1/2) > 0$. This shows that $Q > 0$ on $(0,1)^2$. The rest of the proof is as in the previous case. ♠

6.4 Confining the Vertices

Now we prove Statement 1 of the Voronoi Structure Lemma. In view of the structural results we have proved above, we can say the following about the vertices of VH_p.

1. When $p \in \Upsilon_0$ the vertices are $(163;p),\ (168;p),\ (346;p),\ (189;p)$.
2. When $p \in \Upsilon_1$ the vertices are $(831;p),\ (836;p),\ (189;p),\ (346;p)$.
3. When $p \in \Upsilon_3$ the vertices are $(834;p),\ (839;p),\ (139;p),\ (468;p)$.
4. When $p \in \Upsilon_2$ the vertices are amongst the 8 total listed for Υ_1 and Υ_3.

Note that these vertices might not be distinct for points in the boundaries of these various triangles. Some of the triple points can coalesce. In §8.3 we explain how we compute these points in all cases.

As in §8.3 we introduce the map $L : \boldsymbol{C} \to \boldsymbol{R}^3$ given by

$$L(x+iy) = (x, y, 1). \tag{28}$$

If 3 complex numbers a, b, c are collinear then

$$\det(a,b,c) := L(a) \cdot (L(b) \times (L(c)) = 0. \tag{29}$$

We check, for one point p_0, p_1, p_2, p_3 respectively in each of $\Upsilon_0, \Upsilon_1, \Upsilon_2, \Upsilon_3$ that all the corresponding vertices listed above lie in Δ. We just have to see that this situation cannot change as we vary p around each triangle. Let $\ell \in \{0,1,2,3\}$ be any index. Let t_p be any triple point above associated to Υ_ℓ. Let v, w be any two vertices of the triangle Δ. We consider the function

$$P(p) = \det(t_p, v, w). \tag{30}$$

It suffices to prove that $\epsilon P \geq 0$ on Υ_ℓ for some choice of sign $\epsilon \in \{-1, 1\}$.

For this purpose we consider the function $Q = P \circ F_\ell$. We show that the two functions $\epsilon Q(x/2, y)$ and $\epsilon Q(1 - x/2, y)$ are positive dominant for one of the two choices of sign – the same choice in each case. This proves that $\epsilon Q \geq 0$ on $[0,1]^2$ and hence $\epsilon P \geq 0$ on Υ_ℓ. There are $60 = 3\times 4 + 3\times 4 + 3\times 8 + 3\times 4$ functions in total, and we make the check in each case. This completes the proof.

Remark: We might have taken more effort, as in the previous chapter, to pick our signs in advance so that $\epsilon = 1$ in all cases, but we do not really need to bother with this. Our function checks that either Q is positive dominant or Q is negative dominant by taking the maxima and minima of all the coefficient sums that arise in the definition, and then it checks that the max and the min do not have opposite signs. This suffices.

6.5 Comparing the Distances

In this section we prove Statement 2 of the Voronoi Structure Lemma. Our proof here is almost exactly the same as what we did for the Comparison Lemma. First of all, we check for some choice of p in each triangle $\Upsilon_0, \Upsilon_1, \Upsilon_2, \Upsilon_3$ that

$$|(ijk;p) - p_i| < |(ijk;p) - p_\ell|, \qquad \ell \in \{0,2,5,7\}. \tag{31}$$

Here p_ℓ is one of the vertices of the decagon D_p which is not a vertex of the hexagon H_p and $(ijk;p)$ is one of the triple points above associated to the relevant triangle. We mean to say that we check all possibilities for all triangles. This makes for $80 = 4 \times 4 + 4 \times 4 + 8 \times 4 + 4 \times 4$ checks.

Equation 31 is perhaps stronger than Statement 2 of the Voronoi Structure Theorem because perhaps some of the distances on the right hand side do not correspond to geodesic segments in the dodecahedron connecting the 2 relevant points. Also, the point $(ijk;p)$ might not actually be a vertex of VH_p. None of this bothers us. We will establish Equation 31 for all relevant indices and for all points in the interiors of our triangles. By continuity, we still have a weak inequality even for boundary points. Hence, Equation 31 holds for all p in the relevant triangle provided that $(<)$ is replaced by $(\leq)$. This still implies Statement 2 for all points in the triangle.

Here are the calculation details. As p varies around one of the triangles, Equation 31 fails only if the 4 points (p_i, p_j, p_k, p_ℓ) become cocircular. As in the previous chapter, we let P be the imaginary part of the cross ratio of these points and we let Q be the numerator of $P \circ F$, where F is the relevant triangle map. For each of the 80 choices of Q we check that the functions $\epsilon Q(x/2, y)$ and $\epsilon Q(1 - x/2, y)$ and $\epsilon Q(1/2, y)$ are solidly positive dominant for one of the two choices $\epsilon \in \{-1, 1\}$. This proves that $\epsilon Q > 0$ on $(0,1)^2$. Since Q never vanishes on $(0,1)^2$, we never lose the inequality in Equation 31. This completes the proof.

6.6 Proof of the Selection Lemma

In this section we deduce the Selection Lemma from the Voronoi Structure Lemma. Our argument refers to Figure 6.2, which shows VH_p for some randomly chosen $p \in \Delta$ superimposed over the plan P from Figure 3.1. The reader can see much better pictures of this using my program. The right side of Figure 6.2 is a close-up of the left side.

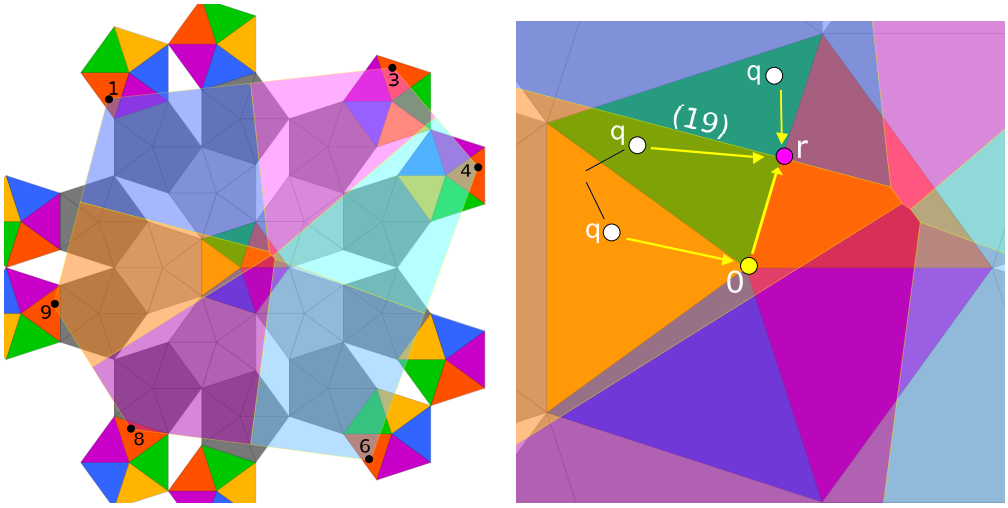

Figure 6.2: The set VH_p superimposed over the dodecahedral plan P.

We parametrize the bisector b_{19} so that we start at ∂H_p, to the left of Δ, and move rightwards. By the Voronoi Structure Lemma, b_{19} eventually intersects Δ, and therefore first hits Δ somewhere in the left edge. This intersection point is r in Figure 6.2.

Let $\omega^k\Delta$ be the triangle obtained from Δ by multiplying to ω^k. Here $\omega = \exp(2\pi/5)$. Let $q \in \widehat{\mathcal{G}}_p$. We want to rule out the possibility that $q \in \omega^k\Delta - \Delta$ for $k = 1, 2, 3, 4$. By symmetry, it suffices to consider $\omega\Delta$ and $\omega^2\Delta$. These are respectively the green and orange central triangles in Figures 3.1 and 6.2. Let Δ_j denote the red triangle in Figure 6.2 containing the point p_j. (This point is just denoted by a j in the figure.)

Case 1: Every point in $\omega\Delta$ can be joined to every point of Δ_1 and to every point of Δ_9 by line segments which remain inside the dodecahedron plan P. Such segments therefore correspond to straightforward geodesic segments joining q to $A(p)$ in the dodecahedron. Thus, if $q \in \omega\Delta$, we have

$$\widehat{d}_X(p, A(q)) = \widehat{d}_X(q, A(p)) \le \min(|q - p_1|, |q - p_9|) = \phi_{19}(q) \qquad (32)$$

The first equality just comes from antipodal symmetry. The last equality is our way of defining the function ϕ_{19}.

Since $q \in \omega\Delta - \Delta$ we have $\phi_{19}(q) < \phi_{19}(r)$. We have the inequalities

$$\widehat{d}_X(p, A(q)) \leq \phi_{19}(q) < \phi_{19}(r) = \mu_{H_p}(r) = \widehat{d}_X(p, A(r)). \tag{33}$$

This contradicts that $q \in \widehat{\mathcal{F}}_p$. The first equality comes from the fact, thanks to the Voronoi Structure Theorem, that b_{19} encounters no triple points until it reaches Δ. Thus $r \in C_1 \cup C_9$, the union of these two Voronoi cells.

The last equality in Equation 33 needs some more justification. Since $r \in H_p$, every line segment joining r to a vertex of H_p lies in the plan P and thus is the developing image of a straightforward geodesic segment which joins r to $A(p)$. Let γ be the shortest of these and let $\ell(\gamma)$ denote its length. By construction

$$\mu_{H_p}(r) = \ell(\gamma).$$

Now, any other straightforward geodesic segment joining r to $A(p)$ corresponds to some line segment connecting r to one of the vertices of the decagon Q_p. But Statement 2 of the Voronoi Structure Theorem says that such segments are no shorter than γ. Hence γ is a shortest straightforward geodesic connecting r to $A(p)$. Hence

$$\widehat{d}_X(r, A(p)) = \ell(\gamma)$$

as well. By symmetry, the same is true for $d_X(p, A(r))$.

Case 2: Now we treat the case $k = 2$. Every point of $\omega^2\Delta$ can be joined to every point of Δ_9 by a line segment that remains inside the plan P. Hence

$$\widehat{d}_X(p, A(q)) \leq |q - p_9| = \phi_9(q). \tag{34}$$

Since $q \notin \Delta$ we have $\phi_9(q) < \phi_9(0)$. Here 0 is the yellow dot on the right side of Figure 6.2. If we drop a perpendiclar from p_9, an arbitrary point of Δ_9, to the line extending the left edge of Δ, the intersection point lies below Δ. Hence $\phi_9(0) \leq \phi_9(r)$. But now we have

$$\widehat{d}_X(p, A(q)) \leq \phi_9(q) < \phi_9(0) \leq \phi_9(r) =^* \phi_{19}(r) = \mu_{H_p}(r) = \widehat{d}_X(p, A(r)). \tag{35}$$

The starred equality comes from the fact that $r \in b_{19}$. The last two inequalities are the same as in Equation 33. We get the same contradiction as in Case 1.

7 The Vertex Competition

7.1 The Competition Lemma

In this section we prove the Competition Lemma. Let us take stock of what we know so far. As in the previous chapters we take

$$p \in \Upsilon_0 \cup \Upsilon_1 \cup \Upsilon_2 \cup \Upsilon_3 = \Upsilon_0 \cup \Sigma_1.$$

What we know so far is that $\widehat{\mathcal{G}}_p$ is always an essential vertex of the Voronoi decomposition VH_p. The possibilities are listed in §6.4. Also, for each of these points $q = (ijk; p)$ we know that the distance from q to $A(p)$ is given by

$$\mu_{H_p}(q) = \min_{j \in \{1,3,4,6,8,9\}} |q - p_j|.$$

We are done with the decagon, so we set $\mu_p = \mu_{H_p}$.

Lemma 7.1 *Let $p \in \Upsilon_0$.*

1. *The point $(189; p)$ belongs to $\widehat{\mathcal{G}}_p$ only if $(189; p) = (168; p)$.*
2. *The point $(346; p)$ belongs to $\widehat{\mathcal{G}}_p$ only if $(346; p) = (163; p)$.*

Proof: Consider the first statement. We show $\mu_p((168; p)) > \mu_p((189; p))$ whenever these points are distinct. Since 1 is an index for both points, this is the same as showing that $|p_1 - (168; p)| > |p_1 - (189; p)|$ whenever the two points are distinct. The two points $(168; p)$ and $(189; p)$ both lie along the bisector b_{18} associated to p. Looking at Figure 3.1 or Figure 6.2 we see that the line $\overline{p_1 p_8}$ lies entirely to the left of the central pentagon Π and in particular entirely to the left of Υ_0. As we travel rightward along b_{18} away from $\overline{p_1 p_8}$ we increase the distance to p_1 (and to p_8). Our rightward travel brings us first to $(189; p)$ and then to $(168; p)$. Hence the latter point is farther from p_1.

Exactly the same argument, with b_{36} replacing p_{18}, and *right* replacing *left*, establishes the second statement. ♠

Lemma 7.2 *Let $p \in \Sigma_1$.*

1. *The point $(139; p)$ belongs to $\widehat{\mathcal{G}}_p$ only if $(139; p) = (839; p)$.*

2. *The point* $(468;p)$ *belongs to* $\widehat{\mathcal{G}}_p$ *only if* $(468;p) = (834;p)$.

3. *The point* $(189;p)$ *belongs to* $\widehat{\mathcal{G}}_p$ *only if* $(189;p) = (831;p)$.

4. *The point* $(364;p)$ *belongs to* $\widehat{\mathcal{G}}_p$ *only if* $(364;p) = (836;p)$.

Proof: This has the same kind of proof as Lemma 7.1. The key points are that lines $\overline{p_3p_9}, \overline{p_4p_8}, \overline{p_1p_8}, \overline{p_3p_6}$ respectively lie above, below, left of, and right of, Σ_1. ♠

We use these lemmas to prove the Competition Lemma. From the Vertex Lemma, we know that when $p \in \Upsilon_0$, the set $\widehat{\mathcal{G}}_p$ is contained in the union of 4 triple points listed in §6.4 in connection with Υ_0. Lemma 7.1 eliminates two of these, leaving the two listed in Statement 2 of the Competition Lemma. Statement 3 follows from Statement 2 and from symmetry.

Statement 4 follows from Lemma 7.2 in the same way that Statement 2 follows from Lemma 7.1.

Now we turn to Statement 1. Our analysis above eliminates all vertices of the Voronoi decomposition VH_p except those incident to the edge e_{16} (in Σ_0) and the edge e_{38} (in Σ_1) which we analyzed in §6.2. A direct calculation shows that when we approach the $\partial\Sigma_0$ the edge e_{16} shrinks to a point and when we approach $\partial\Sigma_1$ the edge e_{38} shrinks to a point. But this combines with Statements 1-3 to show that $\widehat{\mathcal{G}}_p = \{p\}$ in all cases.

Each of the triple points listed in the Competition Lemma does actually arise as a member of $\widehat{\mathcal{G}}_p$ for suitable choices of p. So, it only remains to analyze how the placement of p inside the two states Σ_0 and Σ_1 determines the triple with the largest μ_p-value. After a preliminary section which makes some definitions we need, we treat the two states in turn.

7.2 Preliminaries

To help us analyze the dependence $\widehat{\mathcal{G}}_p$ on the point p, we consider the function from Equation 19. Here it is again.

$$f_{ijk\ell} = |(ijk,p) - p_i|^2 - |(ij\ell,p) - p_i|^2, \tag{36}$$

Suppose we are in some open set U where $f_{ijkl} > 0$ throughout U. This means that $\widehat{\mathcal{G}}_p$ cannot contain $(ij\ell;p)$ when $p \in U$. If $f_{ijkl}(p) = 0$ for some

$p \in U$ it means that $\widehat{\mathcal{G}}_p$ either contains both $(ijk;p)$ and $(ij\ell;p)$ or neither of them. Finally, if $f_{ijkl} < 0$ throughout U it means that $\widehat{\mathcal{G}}_p$ cannot contain $(ijk;p)$ when $p \in U$.

Given Statement 1 of the Competition Lemma, we already know what happens on $\partial\Sigma_0$ and $\partial\Sigma_1$. So, we will work with the open regions Υ_0^o and Σ_0^o. Restricting our attention to Υ_0^o ignores one part of the space, namely the hypotenuse of Υ_0. For ease of exposition, we do not specially treat this edge. The behavior of $\widehat{\mathcal{G}}$ on this edge is just the continuous extension of the behavior in Υ_0^o.

For the indices of interest to us, the function $f_{ijk\ell}$ always factors into smaller factors, one of which is a cubic function $g_{ijk\ell}$. The cubic determines the interface between the cities C_{ijk} and $C_{ij\ell}$. In all but one case, the other factors are linear, and we know them from geometric reasoning: Our function $f_{ijk\ell}$ vanishes on two of the edges on the boundary of the domain of interest, and the defining functions for the lines extending these edges are the linear factors. In one case $h_{ijk\ell}$ factors into two cubics and the other cubic $h_{ijk\ell}$ turns out to be nonzero on the domain. I do not understand this other cubic geometrically.

We also mention a shortcut. Sometimes we do not need to compute f but rather can get g by more direct means. We consider one of the two examples where this applies. Given the structure of VH_p, the points $(831;p)$ and $(839;p)$ are not both essential vertices unless they are equal. So, instead of using the function f_{8319} above we can directly compute the function g_{8319} which is the imaginary part of the cross ratio of (p_8, p_3, p_1, p_9). Similar remarks apply for the quadriple $(8,3,4,6)$.

The analysis in Σ_0, which just involves g_{1638}, is pretty straightforward. We concentrate here on Σ_1. The analysis in Σ_1 is harder because we do not have the same bilateral symmetry. We say that a smooth function g is *cleanly* related to Σ_1 if

1. Some directional derivative of g is nonzero throughout Σ_1.

2. g vanishes on exactly two points of $\partial\Sigma_1$.

If g is cleanly related to Σ_1 then the 0-set γ of g intersects Σ_1 in a single smooth arc which has two points on the boundary.

For Property 1, we will try to use the direction parallel to the segment foliation in Σ_1. These segments are parallel to the line $y = -\tan(\pi/5)x$. We

call this the *preferred direction*. If we can't get the preferred direction to work, we will use the direction $(1,1)$.

We use one of two methods to check Property 2. One approach, the *calculus approach*, is to check that the directional derivatives of g along the directions parallel to the sides of Σ_1 do not vanish in $[0,1]^2$. In these cases, g vanishes at most once in each edge of $\partial\Sigma$, but the level curve can only connect up two of these points. Hence g vanishes only twice on $\partial\Sigma_1$. The other approach, the *restriction method* is that we check explicitly that that g is nonzero on $\partial\Sigma$ except at a pair of vertices of $\partial\Sigma_0$. In this case, γ connects two vertices of Σ_1.

7.3 The Zeroth State

We consider the picture in Υ_0^o. In light of the Competition Lemma, we have the following implications.

1. $f_{1638}(p) > 0$ implies that $\widehat{G}(p) = (163, p)$.
2. $f_{1638}(p) < 0$ implies that $\widehat{G}(p) = (168, p)$.
3. $f_{1638} = 0$ implies that $\widehat{\mathcal{G}}_p \subset \{(163,p),(168,p)\}$.

We mention that the vertical boundary of Σ_0 lies in the solution to the equation $x = \cos(2\pi/5)$. The segment foliation in Σ_0 (and in Υ_0 by restriction) is parallel to the line L whose equation is $y = x\tan(\pi/5)$. Using the formulas from §8.4 we compute in Mathematica that

$$f_{1638}(x,y) = C \times (x - \cos(2\pi/5)) \times y \times g_{1638}, \tag{37}$$

where C is some constant of no interest to us. In other words, f_{1368} vanishes along the horizontal and vertical sides of Υ_0. The nontrivial factor, g_{1638}, is a cubic function which is positive on the interior of the vertical edge of Υ_0, negative on the horizontal edge of Υ_0. We list the formula for g_{1638} in §8.4.

The directional derivative of g_{1638} in the direction of L never vanishes in Σ_0. Numerically, we have

$$\psi = \partial_L(g_{1638}) = \nabla g_{1638} \cdot (\cos(\pi/5), \sin(\pi/5)) \approx$$

$$-38.5375 - 4.10995x + 6.65003x^2 - 2.16073y + 6.99226xy + 6.65003y^2.$$

One can see the non-vanishing from these numerics: $\Sigma_0 \subset [0,1]^2$ and the constant term is much more negative than any of the other terms.

From the structure just discussed, we conclude that the algebraic curve

$$\gamma_{1368} = \{g_{1638} = 0\} \cap \Upsilon_0$$

separates Υ_0 into the cities C_{163} and C_{168} in the combinatorial pattern shown in Figure 1.4, such that each segment in the foliation of Σ (which is parallel to L) intersects the curve exactly once. This gives the claimed decomposition of Υ_0 into cities. When $p \in \gamma_{1638}$, we have the third option listed above, and our two maps are inverses of each other.

We are done with Υ_0. Now let us consider the picture in the bigger domain Σ_0. Let ρ denote the reflection in L. By symmetry, we have similar results for $p \in \rho(\Upsilon_0^o)$, with the indices $4, 9$ replacing the indices $3, 8$. Also by symmetry, we have $(163, p) = (164, p)$ and $(168, p) = (169, p)$ for $p \in L$. This gives us the desired result even when $p \in L \cap \Sigma_0^o$. Finally, by symmetry, the combinatorial pattern of the cities in $\rho(\Upsilon_0)$ is just obtained from the pattern in Υ_0 and reflecting it across L. This is as in Figure 1.4. Hence Theorem 1.2 describes $\widehat{\mathcal{G}}$ for all points in the state Σ_0.

7.4 The First State

We will give the analysis of the picture in Σ_1 modulo some technical lemmas which we prove in the next section. Let L be the line $y = -\tan(\pi/5)x$. This is the direction parallel to the line segment foliation of Σ_1. Let $\mathcal{L}$ denote the segment foliation.

Reflection in the real axis has the following effect on the cities $C_{168} \leftrightarrow C_{831}$ and $C_{163} \leftrightarrow C_{836}$. For this reason,

$$f_{8316}(x,y) = f_{1638}(x,-y), \qquad g_{8316}(x,y) = f_{1638}(x,-y). \tag{38}$$

What we mean is to say that f_{8316} factors just as f_{1638} does, and the cubic factor g_{8316} satisfies the identity just given. We use the cross ratio method to compute g_{8319}, as we already discussed.

Lemma 7.3 *The functions g_{8316} and g_{8319} are cleanly related to Σ_1 and their gradients are linearly independent at each point of Σ_1.*

Proof: See §7.5. ♠

The level curve γ_{8319} intersects $\partial\Sigma_0$ at the $(1,0)$ and at the vertex opposite $(1,0)$. In particular, the endpoints of γ_{8316} and γ_{8319} are interlated on $\partial\Sigma_1$. This means that γ_{8316} and γ_{8319} intersect at least once. Given the properties in the previous lemma, these two curves intersect exactly once in Σ_1.

Now we can say that the subset where $g_{8316} > 0$ and $g_{8319} > 0$ is a simply connected domain bounded by 1 line segment and 2 cubic curves. This counts as a city. We call this city C_{831}. We check that the sign of g_{8319} is correct in the sense that $g_{8319} > 0$ implies that $(831; p)$ rather than $(839; p)$ is the essential vertex of VH_p. From all this, we conclude that

- $G(p) = (831, p)$ for $p \in C^o_{831}$.
- $\widehat{\mathcal{G}}_p$ does not contain $(831, p)$ when $p \in \Sigma_0 - C_{831}$.
- $(831, p) = (839, p)$ along γ_{8319}.

Figure 7.1 shows C_{831} in red.

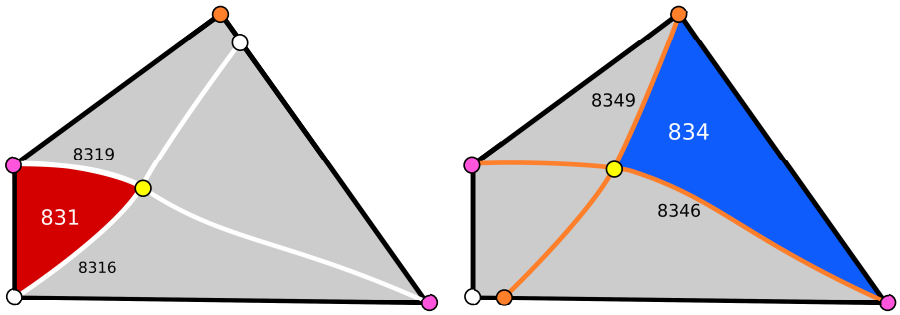

Figure 7.1: The cities C_{831} and C_{834} cut out by intersecting curves.

We define g_{8349} and g_{8346} in the same way, respectively, just as we defined g_{8316} and g_{8319}.

Lemma 7.4 *The functions g_{8349} and g_{8346} are cleanly related to Σ_1 and their gradients are linearly independent at each point of Σ_1.*

Proof: This has the same proof as Lemma 7.3. ♠

We define C_{834} just as we defined C_{831}. From the structure above we conclude the following:

- $G(p) = (834, p)$ for $p \in C^o_{834}$.

- $\widehat{\mathcal{G}}_p$ does not contain $(834, p)$ when $p \in \Sigma_0 - C_{834}$.
- $(834, p) = (836, p)$ along γ_{8346}.

Figure 7.1 draws C_{834} in blue. We have drawn these cities as disjoint. We will justify the disjointness at the end.

We have $\widehat{\mathcal{G}}_p \subset \{(836, p), (839, p)\}$ for $p \in \Sigma_0^o - C_{831} - C_{834}$. The function f_{8369} is the most complicated one we need to consider. After a lot of *ad hoc* work on Mathematica, I found that $f = gh$ where g_{8369} and h_{8369} are both cubics. The formula for h_{8369} is given in Equation 56, and the reader can verify that indeed $f = gh$. I don't have a geometric understanding of h_{8369}.

Lemma 7.5 *h_{8369} is positive on Σ_1^o and cleanly related to Σ_1.*

Proof: See §7.5, ♠

Thus, g_{8369} determines the competition between $(836; p)$ and $(839; p)$ in Σ_1. Let γ_{8369} be the zero level curve in Σ_1 associated to g_{8369}.

Lemma 7.6 *γ_{8369} intersects each of $\gamma_{8316}, \gamma_{8319}, \gamma_{8346}, \gamma_{8349}$ exactly once.*

Proof: See §7.5. ♠

Now let us analyze the locations of the intersection points. The intersection point $\gamma_{8369} \cap \gamma_{8319}$ must lie on the curve γ_{8319} because, as we have already mentioned, we have $(831, p) = (836, p)$ at this point. Hence γ_{8369} intersects C_{831} at its interior vertex. Likewise γ_{8369} intersects C_{834} at its interior vertex.

Consider the arc

$$\beta = \gamma_{8316} \cup \gamma_{8369} \cup \gamma_{8319}. \tag{39}$$

This is the red-blue interface on the right side of Figure 1.4.

Lemma 7.7 *The arc β is embedded and joins the origin to the opposite vertex of Σ_1. Moreover, each segment of $\mathcal{L}$ meets β exactly once.*

Proof: Each of the three arcs of β is embedded, and the middle arc intersects the other two exactly once. To show that β is embedded, it suffices to prove that γ_{8316} and γ_{8319} are disjoint. Recall that each segment of $\mathcal{L}$. meets each

of these arcs at most once. We just have to show that no segment of $\mathcal{L}$ meets both arcs.

The segments of $\mathcal{L}$ have a *transverse order*: We order them according to the y-intercepts of the lines extending these segments. The two vertices of β are $b_1 = \gamma_{8316} \cap \gamma_{8369}$ and $b_2 = \gamma_{3869} \cap \gamma_{8319}$. As we move along γ_{8369} away from the origin and transverse to the segments in $\mathcal{L}$, we encounter b_1 before b_2. Hence, all the segments of $\mathcal{L}$ which meet γ_{8316} precede, in the transverse order, all the segments of $\mathcal{L}$ which meet γ_{8319}. This establishes the claim that β is embedded.

We check that g_{8316} vanishes at the origin and locally takes opposite signs on the edges of Σ_1 incident to the origin. Hence γ_{8316} has one endpoint at the origin. Call the origin v_0. Similarly, γ_{8319} has one endpoint at the vertex v_1 of Σ_1 opposite the origin. Hence β is an embedded arc joining v_0 to v_1.

From what we have said above, each segment of $\mathcal{L}$ meets β at most once. Since β joins a pair of opposite vertices of Σ_1 and since every segment of $\mathcal{L}$ meets both components of $\partial\Sigma_1 - \{v_0, v_1\}$, we see that every segment of $\mathcal{L}$ meets β. Hence every segment of $\mathcal{L}$ meets β exactly once. ♠

Corollary 7.8 *C_{831} and C_{834} are disjoint.*

Proof: Each of these cities shares an arc with β and hence lies in one component of $\Sigma_1 - \beta$. We check that the one city lies in one component and the other city lies in the other component. ♠

Our results above give us the combinatorial picture shown on the right side of Figure 1.4. We have established all the claimed properties about the cities in Σ_1. This establishes that the dynamical system in Theorem 1.2 describes $\widehat{\mathcal{G}}$ in the state Σ_1.

7.5 Technical Details

Now we prove the lemmas whose we deferred in the previous section. For convenience we repeat the lemmas.

Lemma 7.9 *The functions g_{8316} and g_{8319} are cleanly related to Σ_1 and their gradients are linearly independent at each point of Σ_1.*

Proof: We check that $\partial_L g_{8316}$ does not vanish in $[0,1]^2$, a region which contains Σ_1. This is Property 1 above. We use the calculus method to check Property 2 for g_{8316}. The method works in an obvious way, with the constant term dominating the others, as it did for g_{1638} above.

Now we consider g_{8319}. Let $\psi = \partial_{(1,1)} g_{8319}$. Let F_1, F_2, F_3 be the triangle maps defined in the previous chapter. We check that $\psi \circ F_j$ is strongly positive dominant for $j = 1,2,3$. This checks that ψ does not vanish in Σ_1. This is Property 1. We use the evaluation method to check Property 2 for g_{8319}.

Let

$$g = \det(\nabla g_{8316}, \nabla g_{8319}).$$

This function vanishes if and only if two gradients are parallel. We check that the 3 functions $g \circ F_j$ are strongly positive dominant. This does it. ♠

Lemma 7.10 *h_{8369} is positive on Σ_1^0 and cleanly related to Σ_1.*

Proof: Let F_1, F_2, F_3 be the same triangle maps above. For each polynomial $Q_j = h_{8369} \circ F_j$ and some sign choice ϵ_j we check that the 8 functions

$$\epsilon_j Q_j(x/2, y/2),\ \epsilon_j Q_j(1-x/2, y/2),\ \epsilon_j Q_j(x/2, 1-y/2),\ \epsilon_j Q_j(1-x/2, 1-y/2),$$

$$\epsilon_j Q_j(1/2, y/2),\ \epsilon_j Q_j(1/2, 1-y/2),\ \epsilon_j Q_j(x/2, 1/2),\ \epsilon_j Q_j(1-x/2, 1/2)$$

are solidly positive dominant. We also check that $\epsilon_j Q_j(1/2, 1/2) > 0$ in all 3 cases. This shows that h_{8369} is positve on Σ_1^o.

We check the preferred directional derivative $\partial_L g$ and we use the calculus method for the other 4 directions. In all cases, the constant term is much larger than the other terms and the result is numerically obvious. ♠

Lemma 7.11 *γ_{8369} intersects each of γ_{8316} and γ_{8319} once.*

Proof: The proof is the same in both cases. We give the proof for γ_{8316}. We check that the endpoints are interlaced, so we just have to verify the gradient condition. The gradient condition does not quite work, so we have to scramble.

Consider the function g_{8319}. We note that $\Sigma_1 \subset [0,1] \times [0,1/2]$. We check that $\epsilon g_{8369}(1 - x/4, y/2)$ is strongly positive dominant for some sign choice ϵ. This means that $g_{8369} \neq 0$ on $[3/4,1] \times [0,1/2]$. Hence

$$\gamma_{8369} \subset [0,3/4] \times [0,1/2].$$

We set $\psi = \det(\nabla g_{8369}, \nabla g_{8316})$ and check that $\psi(3x/4, y/2)$ is positive dominant. This shows that the two gradients are linearly independent in the rectangle $[0,3/4] \times [0,1/2]$. Hence γ_{8369} and γ_{8316} intersect exactly one. ♠

Lemma 7.12 *γ_{8369} intersects γ_{8346} and γ_{8349} once each.*

Proof: The proof is the same in both cases. We give the proof for γ_{8346}. The endpoints in each case are interlaced and so we just have to check the linear independence of the gradients. We observe that $\Sigma_1 \in R = [3/10,1] \times [0,1/2]$ so we just have to check the linear independence in this smaller rectangle. Define $\psi = \det(\nabla g_{8369}, \nabla g_{8346})$. check that $\epsilon\psi(1 - 7x/10, y/2)$ is strongly positive dominant for one of the sign choices. This shows that ψ does not vanish on R. ♠

8 Formulas

8.1 Transplant Codes

This section concerns chains whose sequence ends in 11. These correspond to geodesic segments which connect a point in Π with a point in $A(\Pi)$. Given a chain C there is a 6 digit *transplant code* $(c_0, ..., c_5)$ with the following property. Given $p \in \Pi$ the point $A(p) \in A(\Pi)$ develops out to the point

$$\langle C, p \rangle = \sum_{k=0}^{4} c_k \exp(2\pi i k/5) + \exp(\pi i c_5/5)\overline{p}. \tag{40}$$

Here, as usual, we identity Π with the pentagon in $\boldsymbol{C}$ whose vertices are the 5th roots of unity. We call $\langle C, p \rangle$ the *transplant* of p with respect to C.

In our proof of the Correspondence Lemma, we considered $6 + 60$ chains. The first 6 chains let us define the vertices $p_1, p_3, p_4, p_6, p_8, p_9$ of the hexagon H_p. The other 60 chains are the competing chains which we eliminate. The point p_j is give by $\langle c_j, p \rangle$, where

- $c_1 : (0, 3, 3, 1, 0, 7)$.
- $c_3 : (3, 3, 1, 0, 0, 3)$.
- $c_4 : (3, 3, 0, 0, 1, 1)$.
- $c_6 : (3, 0, 0, 1, 3, 7)$.
- $c_8 : (0, 0, 1, 3, 3, 3)$.
- $c_9 : (0, 0, 3, 3, 1, 1)$.

Here we 6 of the sequences corresponding to the 60 competing chains and the corresponding transplant codes.

- $0, 2, 1, 9, 11 \to 2, 4, 3, 0, 1, 4$
- $2, 10, 9, 11 \to 1, 4, 3, 2, 0, 6$
- $0, 3, 2, 9, 11 \to 1, 3, 4, 2, 0, 6$
- $0, 3, 10, 9, 11 \to 0, 2, 4, 3, 1, 8$

- $0, 3, 2, 10, 9, 11 \to 2, 2, 5, 3, 0, 7$
- $0, 4, 3, 10, 9, 11 \to 0, 2, 3, 5, 2, 9$.

We can deduce the remaining transplant codes by symmetry. Given a chain C we define $C^{\#}$ to be the mirror image of C. We define ωC to be the chain whose developing image is obtained from that of C by multiplying the whole picture by $\exp(2\pi i/5)$. For instance if the sequence associated to C is $0, 2, 9, 11$ then the sequence associated to ωC is $0, 3, 10, 11$. Given any chain C we have the 10 chains $\omega^k C$ and $\omega^k C^{\#}$ for $k = 0, 1, 2, 3, 4$. We call these new chains the *dihedral images* of C. Here are the rules for figuring out the transplant codes for the dihedral images. Assume that C has transplant code $c_0, ..., c_6$ as above. Then...

1. $C^{\#}$ has transplant code $c_2, c_1, c_0, c_4, c_3, 8 - c_5$.
2. ωC has transplant code $c_4, c_0, c_1, c_2, c_3, c_5 + 4$.

8.2 Triangle Maps

In the proof of the Comparison Lemma and the Voronoi Structure Lemma, we relied on certain polynomial maps from $[0,1]^2$ to certain triangles Υ We call these the *triangle maps*. Here are the domains

1. $\Upsilon_0 = \Upsilon_{1638}$. This contains the cities C_{834} and C_{839}.
2. Υ_{8349}. This contains the cities C_{831} and C_{836}.
3. Υ_{8316}. This contains the cities C_{163} and C_{168}.
4. Υ_1.
5. Υ_2.
6. Υ_3.

Together, $\Upsilon_1, \Upsilon_2, \Upsilon_3$ partition the state Σ_0.

Let Υ be one of the triangles of interest to us. We want to construct a surjective polynomial map $F : [0,1]^2 \to \Upsilon$. In all case let T_0 be the triangle with vertices $(0,0)$, $(1,0)$ and $(1,1)$. We write $F = f_1 \circ f_2$, where

- f_1 is an affine map from the triangle T_0 to Υ.

- $f_2(x,y) = (x, xy)$.

To define F in each case, we just need to write down the affine map f_1 we use in each case. Here are the 6 maps, listed in the same order as the corresponding triangles. The various versions of f_1 send (x,y) to ...

$$\left(\frac{x}{\sqrt{5}+1}, \frac{\sqrt{5-2\sqrt{5}}y}{\sqrt{5}+1}\right). \tag{41}$$

$$\left(\frac{2\sqrt{5}x - \sqrt{5}y + 2}{2\sqrt{5}+2}, \frac{\sqrt{10-2\sqrt{5}}\left(-2x + \left(\sqrt{5}+2\right)y + 2\right)}{4\left(\sqrt{5}+3\right)}\right). \tag{42}$$

$$\left(x + \frac{1}{8}\left(\sqrt{5}-7\right)y, \frac{1}{4}\sqrt{\frac{1}{2}\left(5-\sqrt{5}\right)}y\right), \tag{43}$$

$$\left(\frac{2\sqrt{5}x - \sqrt{5}y + 2}{2\sqrt{5}+2}, \frac{\sqrt{10-2\sqrt{5}}\left(-2x + \left(\sqrt{5}+2\right)y + 2\right)}{4\left(\sqrt{5}+3\right)}\right) \tag{44}$$

$$\left(\frac{-4\sqrt{5}x + \sqrt{5}y - y + 4\sqrt{5} + 4}{4\sqrt{5}+4}, \frac{\sqrt{10-2\sqrt{5}}\left(4x + \left(\sqrt{5}-1\right)y\right)}{8\left(\sqrt{5}+3\right)}\right) \tag{45}$$

$$\left(\frac{1}{8}\left(\left(\sqrt{5}-5\right)x - 2y + 8\right), \frac{1}{16}\sqrt{10-2\sqrt{5}}\left(\sqrt{5}x + x - \sqrt{5}y + y\right)\right) \tag{46}$$

8.3 Triple Points

We will need to compute various triple points $(ijk;p)$ where

$$i,j,k \in \{1,3,4,6,8,9\}.$$

The point $(ijk;p)$ is equidistant from p_i, p_j, p_k. There is a rational expression which computes this, but we prefer to use an alternate approach.

The points

$$p_{ij} = (p_i + p_j)/2, \qquad q_{ij} = p_{ij} + i(p_i - p_j) \tag{47}$$

are both points on the bisector b_{ij}. We likewise define p_{jk} and q_{jk}.

We define maps $L : \boldsymbol{C} \to \boldsymbol{R}^3$ and $P : \boldsymbol{R}^3 \to \boldsymbol{C}$ as follows:

$$L(x+iy) = (x, y, 1), \qquad P(x, y, z) = (x/z, y/z). \tag{48}$$

The map PL is the identity. These maps are familiar from projective geometry.

We have

$$(ijk; p) = P\Big((L(p_{12}) \times L(q_{12})) \times (L(p_{23}) \times L(q_{23})) \Big). \tag{49}$$

Here $(\times)$ denotes the vector cross product.

8.4 Formulas for the City Boundaries

We give formulas for the curves considered above. Every formula for a city edge can be obtained from the ones below by pre-composing these formulas with a dihedral symmetry of the pentagonn Π. We have the relation $g_{1683}(x, y) = g_{8316}(x, -y)$, so we won't give the formula explicitly for g_{1683}. This leaves us with the quadruples above which begin with 83.

As we mentioned in the introduction, these functions all have the form

$$\sum_{i+j \le 3} \left(s_{ij} \sqrt{a_{ij} + b_{ij}\sqrt{5}} \right) x^i y^j = 0, \qquad s_{ij} \in \{-1, 0, 1\}, \quad a_{ij}, b_{ij} \in \boldsymbol{Z}. \tag{50}$$

We will supply the matrices $\{s_{ij}\}$ and $\{a_{ij}\}$ and $\{b_{ij}\}$ in all the relevant cases. Since it is easy to mix up matrices with their transposes, let me say explicitly that the top horizontal row corresponds to the monomials $1, x, x^2, x^3$. With that said, here is the data for g_{8316}.

$$\begin{bmatrix} + & - & - & + \\ + & + & - & 0 \\ - & + & 0 & 0 \\ - & 0 & 0 & 0 \end{bmatrix} \quad \begin{bmatrix} 50 & 585 & 225 & 60 \\ 283 & 12 & 8 & 0 \\ 25 & 40 & 0 & 0 \\ 8 & 0 & 0 & 0 \end{bmatrix} \quad \begin{bmatrix} 20 & 171 & -99 & -16 \\ 105 & -4 & 0 & 0 \\ 0 & 40 & 0 & 0 \\ 8 & 0 & 0 & 0 \end{bmatrix} \tag{51}$$

Here are the matrices for g_{8349}:

$$\begin{bmatrix} + & - & - & + \\ + & - & + & 0 \\ - & + & 0 & 0 \\ + & 0 & 0 & 0 \end{bmatrix} \quad \begin{bmatrix} 940 & 9480 & 235 & 60 \\ 7780 & 100 & 20 & 0 \\ 75 & 60 & 0 & \\ 20 & 0 & 0 & 0 \end{bmatrix} \quad \begin{bmatrix} 420 & 4400 & 105 & 20 \\ 3476 & 44 & -4 & 0 \\ 25 & 20 & 0 & 0 \\ -4 & 0 & 0 & 0 \end{bmatrix} \tag{52}$$

Here are the matrices for g_{8319}:

$$\begin{bmatrix} 0 & - & + & - \\ + & + & - & 0 \\ - & - & 0 & 0 \\ - & 0 & 0 & 0 \end{bmatrix} \quad \begin{bmatrix} 0 & 85 & 130 & 5 \\ 29 & 206 & 9 & 0 \\ 20 & 5 & 0 & \\ 9 & 0 & 0 & 0 \end{bmatrix} \quad \begin{bmatrix} 0 & 38 & 58 & 2 \\ 12 & 90 & 4 & 0 \\ 8 & 2 & 0 & 0 \\ 4 & 0 & 0 & 0 \end{bmatrix} \tag{53}$$

Here are the matrices for g_{8346}:

$$\begin{bmatrix} 0 & - & + & + \\ + & + & + & 0 \\ - & + & 0 & 0 \\ + & 0 & 0 & 0 \end{bmatrix} \quad \begin{bmatrix} 0 & 126075 & 58835 & 16810 \\ 109265 & 336200 & 16810 & 0 \\ 294175 & 5 & 0 & \\ 16810 & 0 & 0 & 0 \end{bmatrix} \quad \begin{bmatrix} 0 & 42045 & 25215 & 0 \\ 31939 & 26896 & 6724 & 126075 \\ 0 & 2 & 0 & 0 \\ 6724 & 0 & 0 & 0 \end{bmatrix} \tag{54}$$

Here are the matrices for g_{8369}:

$$\begin{bmatrix} + & - & - & + \\ + & + & - & 0 \\ - & + & 0 & 0 \\ - & 0 & 0 & 0 \end{bmatrix} \quad \begin{bmatrix} 4700 & 41160 & 210 & 175 \\ 14180 & 1220 & 5 & 0 \\ 2010 & 175 & 0 & 0 \\ 5 & 0 & 0 & 0 \end{bmatrix} \quad \begin{bmatrix} 2100 & 18400 & 80 & 75 \\ 6316 & 524 & 1 & 0 \\ 880 & 75 & 0 & 0 \\ 1 & 0 & 0 & 0 \end{bmatrix} \tag{55}$$

Here are the matrices for h_{8369}:

$$\begin{bmatrix} 0 & - & + & + \\ + & - & + & 0 \\ - & + & 0 & 0 \\ + & 0 & 0 & 0 \end{bmatrix} \quad \begin{bmatrix} 0 & 196800 & 103040 & 15040 \\ 1056320 & 2044160 & 28480 & 0 \\ 515200 & 15040 & 0 & 0 \\ 28480 & 0 & 0 & 0 \end{bmatrix} \quad \begin{bmatrix} 0 & 88000 & 46080 & 6720 \\ 472384 & 914176 & 12736 & 0 \\ 230400 & 6720 & 0 & 0 \\ 12736 & 0 & 0 & 0 \end{bmatrix} \tag{56}$$

8.5 Formulas for the Special Points

The quadruple point in Σ_0^o is $(\cos(\pi/5)t, \sin(\pi/5)t)$, where $t = 0.25016...$ is a root of the following cubic.

$$(5 + 3\sqrt{5}) + (-24 - 10\sqrt{5})t + (-5 + \sqrt{5})t^2 + 4t^3.$$

In the case of the triple points in Σ_1^o, I don't know how to prove that the formulas I got from Mathematica are correct, but I list them anyway. In the equations below, the list $(a_0, ..., a_{10})$ stands for the polynomial

$$a_0 + a_1 t + ... + a_{10} t^{10}.$$

The two triple points in Σ_1^o are the

$$(\cos(2\pi/5)u_1, \sin(2\pi/5)v_1), \qquad (\cos(2\pi/5)u_2, \sin(2\pi/5)v_2),$$

where u_1, v_1, u_2, v_2 respectively are the roots of the following polynomials.

$$(316255, -1021235, 1187259, 628411, -2861623, 3126530, -1726141, 440390, -15077, -8998, 604).$$

$$(-495, 9045, -59511, 170103, -171269, -112328, 339489, -267720, 108905, -25870, 3020)$$

$$(-1044164, 4232724, -10713465, 20137044, -23128795, 14627289, -5047850, 960889, -66285, -10636, 724)$$

$(-3820, 14590, 3825, -149495, 131854, 97712, -165546, -51200, 15, -10750, 362010)$

To specify the roots exactly it is enough to note that

$u_1 = 1.4799....,$ $v_2 = .21542...,$ $u_2 = 1.4984...,$ $v_2 = .23169...$

These 4 degree 10 polynomials are irreducible, and Sage tells us that their Galois groups are all degree 2 extensions of $S_5 \times S_5$ where S_5 is the symmetric group on 5 symbols. Hence the coordinates for these triple points are not solvable numbers. I also found the polynomials for x_1, y_1, x_2, y_2. The formulas for x_1, x_2 are similar to the ones for u_1, u_2. The formulas for y_1, y_2 are degree 20 even polynomials with enormous integer coefficients.

9 References

[**R1**] J. Rouyer, *Antipodes sur le tétraèdra régulier*, J. Geom. **77** (2003), no. 4, pp. 152-170.

[**R2**] J. Rouyer, *On antipodes on a convex polyhedron*, Adv. Geom. **5** (2005), no. 4, pp. 497-507.

[**R3**] J. Rouyer, *On antipodes on a convex polyhedron II*, Adv. Geom. **10** (2010), no. 3, pp. 403-417.

[**S1**] R. E. Schwartz, *The Farthest Point Map on the Regular Octahedron*, J. Experimental Mathematics, 2021 (to appear).

[**S2**] R. E. Schwartz, *The Projective Heat Map*, A.M.S. Research Monograph (2016)

[**V1**] C. Vılcu, *On two conjectures of Steinhaus*, Geom. Dedicata **79** (2000), no. 3, pp. 267-275.

[**V2**] C. Vılcu, *Properties of the farthest point mapping on convex surfaces*, Rev. Roum. Math. Pures Appl. **51** (2006), no. 1, pp. 125-134.

[**VZ**] C. Vılcu and T. Zamfirescu, *Multiple farthest points on Alexandrov surfaces*, Adv. Geom. **7** (2007), no. 1, pp. 83-100.

[**W**] Z. Wang, *Farthest Point Map on a Centrally Symmetric Convex Polyhedron*, Geometriae Dedicata **204** (2020), pp. 73-97.

[**Wo**] S. Wolfram, *Mathematica* (2020) wolfram.com/mathematica.

[**Z**] T. Zamfirescu, *Extreme points of the distance function on a convex surface*, Trans. Amer. Math. Soc. **350** (1998), no. 4, pp. 1395-1406.